DE LA RECHERCHE À L'INDUSTRIE

Laser-matter interaction from solid to plasma

L.Videau[1,2], P. Combis[1], L. Berthe[3]
S. Bardy[1,2], M. Scius-Bertrand[1,2], A. Rondepierre[3] et al

1. CEA, DAM Ile de France, Bruyères le Châtel, France
2. Laboratoire Matière en Conditions Extrêmes, CEA, Université Paris-Saclay, France
3. Arts et métiers , Institute of Technology , CNRS, CNAM, PIMM, HESAM University, 75013 Paris, France

Motivations : development of a unique laser-matter interaction tool to address different laser applications

Petawatt laser prepulse study

solid – plasma (ps – ns)

N. Zaim (LOA), PoP 26 (2019)
M. Gambari (LP3), thesis (2020)

LASer Adherence Test and Laser Shock Peening

solid – plasma (5-100 ns)

C. LeBras (PIMM), Metals (2019)
S. Bardy (DIF), JOLT (2020)
M. Scius-Bertrand (DIF), JAP (2021)

Laser ablation for spatial applications

solid – plasma
ps - ns

C. Phipps et al, Acta Astro. (2018)

$I = 10^9 – 10^{13}$ W/cm²

Laser-driven cratering experiments

solid – plasma (ns)

G. Seisson (CESTA) IJIE (2014,2016)
B. Aubert (CESTA), JLA (2019)

VISAR blanking

solid – liquid (ns)

G. Debras (DIF), EPJ (2013)
S. Laffite (DIF), PoP 21 (2014)

Laser-plasma experiments interpretation

solid – plasma (ns)

R. Torchio (ESRF) Sci. Rep. (2016)
C. Pepin (DIF) PRB (2020)
A. Denoeud (DIF) RSI (2021)

Outline

- **Laser-matter interaction models for one-dimensional codes**
  - Numerical methods
  - Optical properties
- **Experiments for ablation pressure characterization**
  - Direct interaction in vacuum
  - Confinement regime
- **2D effects**
- **Laser ablation experiments on ELFIE**
- **LAser Shock Adherence Test**

Implementation in the one-dimensional multi-physics ESTHER code (Patrick Combis work from 2006->2017)

- Laser absorption and propagation (Helmholtz equation, raytracing)
- Energy deposition (X-ray, ions)
- Hydrodynamic, mechanics, fracture (Johnson model)
- Thermal conduction (diffusion equation)
- Radiative heat transfer (SN-method)
- Electron-ion coupling (2T model)
- Phase transition model (Hayes, Greeff)
- …

Laser-matter interaction models for Lagrangian codes

Maxwell general equations (non-magnetic)

$$rot(\vec{\mathcal{E}}) = -\frac{\partial \vec{\mathcal{B}}}{\partial t} \quad ; \quad div(\vec{\mathcal{D}}) = \rho$$

$$rot(\vec{\mathcal{H}}) = \frac{\partial \vec{\mathcal{D}}}{\partial t} + \vec{\mathcal{J}} \; ; \quad div(\vec{\mathcal{B}}) = 0$$

Geometrical optics approximation* (λ → 0)

Eikonal equation $\vec{E}(\vec{r}) = \vec{e}(\vec{r})\, e^{ik_0 S(\vec{r})}$

Monochromatic plane wave ($\vec{E}(\vec{r}) = A\, e^{i\vec{k}.\vec{r}}$)

Helmholtz equation $\Delta\tilde{E} + \left(\frac{\omega}{c}\tilde{n}\right)^2 \tilde{E} = 0$

* see A. Colaïtis talk

Method 1 : Helmholtz equation resolution in one-dimensional planar geometry

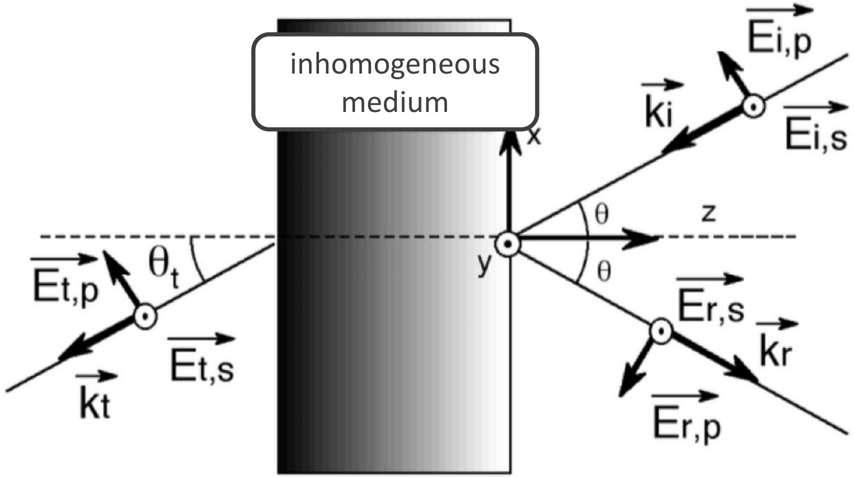

Analytic resolution in each homogenous cell

$$\Delta\tilde{E} + \left(\frac{\omega}{c}\tilde{n}_i\right)^2 \tilde{E} = 0$$

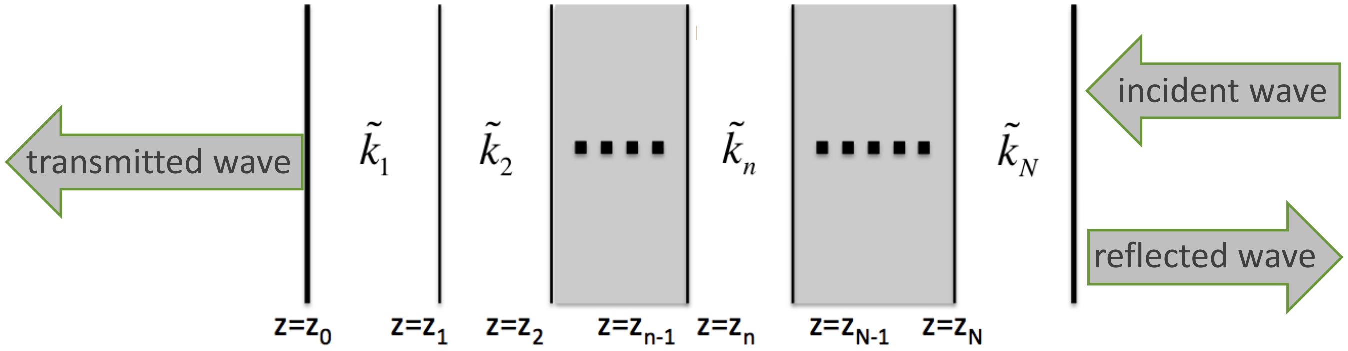

- Analytical resolution in each homogeneous cell
- Boundary conditions at each node to connect analytic solutions
- Numerical calculation (matrix resolution or step-by-step resolution)
- \+ : phase calculation, interference effects, sharp interface possible
- \- : only available in a planar geometry in our Lagrangian code

Method 2 : geometrical optics approximation for one-dimensional planar/cylindrical/spherical geometries

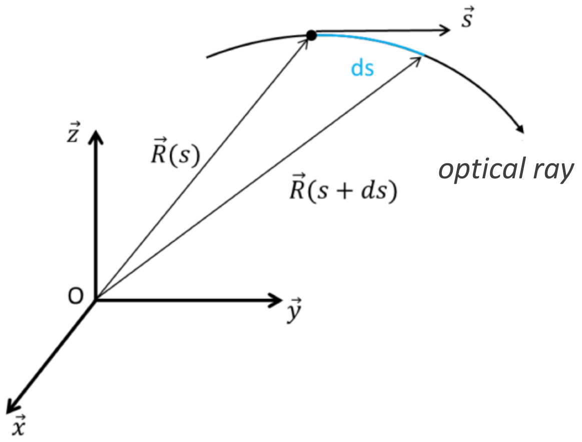

Extension of eikonal equations for metals ($n_1 \rightarrow |n|$)

$$\begin{cases} \dfrac{d^2\vec{R}}{d\tau^2} = \dfrac{1}{2}\overrightarrow{grad}(|n|^2) \text{ avec } n\,d\tau = ds \\ \dfrac{dI}{ds} = -K_{abs}(\omega)I \end{cases}$$

Analytical step-by-step resolution by using linear interpolation for $|n|^2$ and $|n|\,n_2$

$$\begin{cases} u_i = \frac{|\tilde{n}(r)|^2}{2} = a_i r + b_i, \\ v_i = 2\mid \tilde{n(r)} \mid n_2(r) = c_i r + d_i. \end{cases}$$

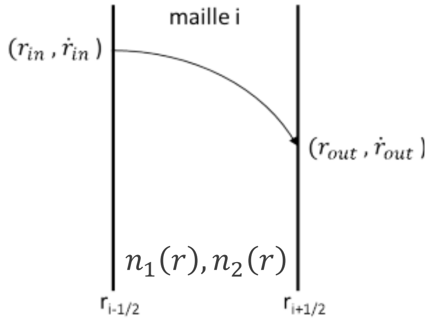

$$\begin{cases} r_{out} = r_{in} + \epsilon_{in} e_i, \\ \dot{r}_{out} = \epsilon_{in}\sqrt{\dot{r}_{in}^2 + 2\epsilon_{in} a_i e_i}, \\ \tau_{out} = \tau_{in} - \frac{\dot{r}_{in}}{a_i} + \frac{1}{\epsilon_{in} a_i}\sqrt{\dot{r}_{in}^2 + 2\epsilon_{in} a_i e_i}, \\ \ln\frac{I_{out}}{I_{in}} = -k_0\frac{c_i}{6a_i^2}(\dot{r}_{out}^3 - \dot{r}_{in}^3) - k_0(c_i r_{in} + d_i - c_i\frac{\dot{r}_{in}^2}{2a_i})(\frac{\dot{r}_{out} - \dot{r}_{in}}{a_i}) \end{cases}$$

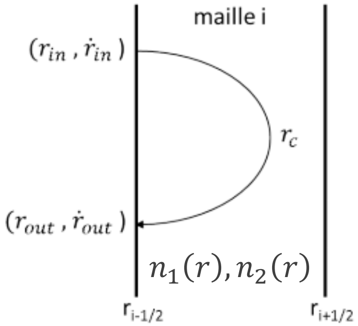

$$\begin{cases} r_{out} = r_{in}, \\ \dot{r}_{out} = -\dot{r}_{in}, \\ \tau_{out} = \tau_{in} - \frac{2\dot{r}_{in}}{a_i}, \\ \ln\frac{I_{out}}{I_{in}} = 2k_0\frac{c_i}{6a_i^2}\dot{r}_{in}^3 + 2k_0(c_i r_{in} + d_i - c_i\frac{\dot{r}_{in}^2}{2a_i})\frac{\dot{r}_{in}}{a_i} \end{cases}$$

*L. Videau, published in Univ. Paris-Saclay, 2020 (tel-03129739)

Construction of analytical unit tests to compare and validate both methods in representative cases

Brekhovskikh L.M. "Waves in layered media" *Applied Mathematics and Mechanics* (1980)

analytical index profile

$$\tilde{n}^2(z) = -a^2\left(K_1 + \frac{1}{4}\right) + \frac{a^2 K_2 e^{ak_0 z}}{1 + e^{ak_0 z}} + \frac{a^2 K_3 e^{ak_0 z}}{(1 + e^{ak_0 z})^2}$$

$$x = -e^{ak_0 z}$$

Helmholtz equation →

$$E(z) = \frac{x^{\gamma/2}}{\sqrt{ak_0 x}}(1-x)^{(\alpha+\beta+1-\gamma)/2} \; {}_2F_1(\alpha;\beta;\gamma;x)$$

$$\begin{aligned}
\alpha &= \frac{1}{2}\left(1 + \sqrt{1+4K_1} + \sqrt{1+4K_3} - \sqrt{1+4(K_1-K_2)}\right)\\
\beta &= \frac{1}{2}\left(1 + \sqrt{1+4K_1} + \sqrt{1+4K_3} + \sqrt{1+4(K_1-K_2)}\right)\\
\gamma &= 1 + \sqrt{1+4K_1} = 1 + \frac{2}{a}i
\end{aligned}$$

symmetric layer (R<1% - A=53%)

(equivalent to a plasma bubble or a jet)

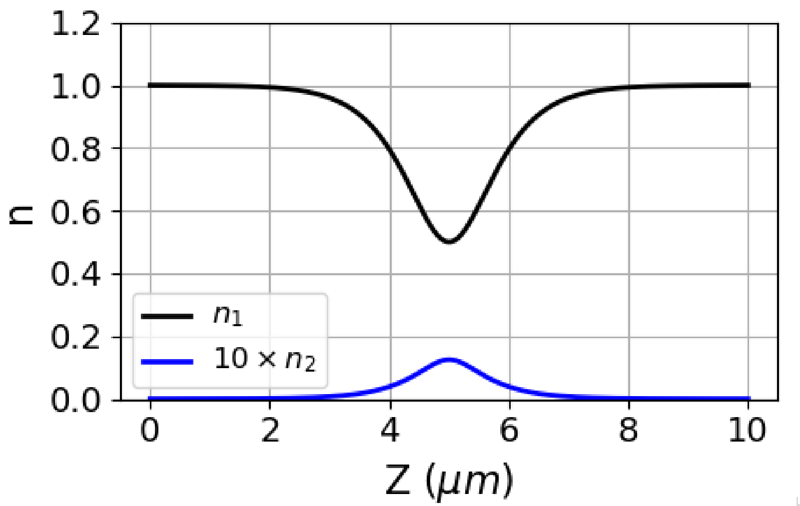

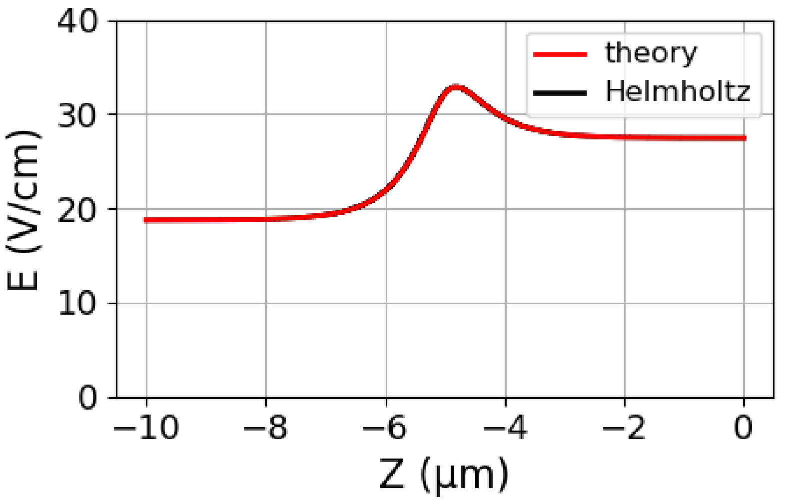

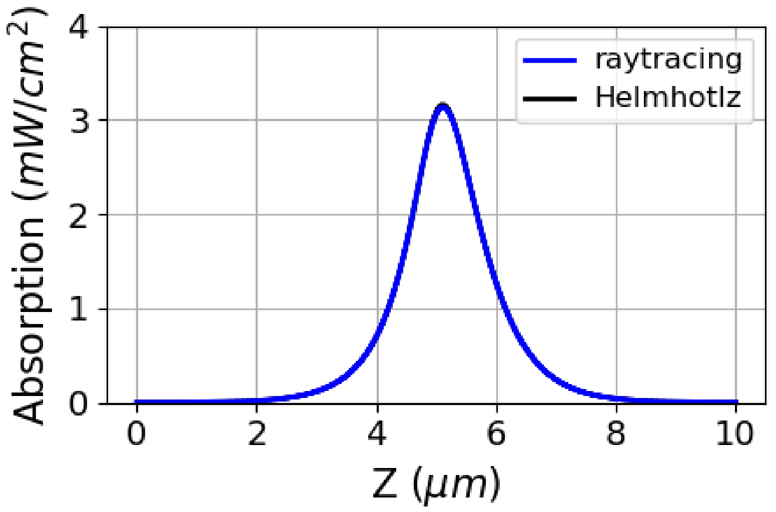

Construction of analytical unit tests to compare and validate both methods in representative cases

Brekhovskikh L.M. "Waves in layered media" *Applied Mathematics and Mechanics* (1980)

analytical index profile

$$\tilde{n}^2(z) = -a^2\left(K_1 + \frac{1}{4}\right) + \frac{a^2 K_2 e^{ak_0 z}}{1+e^{ak_0 z}} + \frac{a^2 K_3 e^{ak_0 z}}{(1+e^{ak_0 z})^2}$$

$$x = -e^{ak_0 z}$$

Helmholtz equation

$$E(z) = \frac{x^{\gamma/2}}{\sqrt{ak_0 x}}(1-x)^{(\alpha+\beta+1-\gamma)/2}\ {}_2F_1(\alpha;\beta;\gamma;x)$$

$$\begin{aligned}
\alpha &= \frac{1}{2}\left(1+\sqrt{1+4K_1}+\sqrt{1+4K_3}-\sqrt{1+4(K_1-K_2)}\right)\\
\beta &= \frac{1}{2}\left(1+\sqrt{1+4K_1}+\sqrt{1+4K_3}+\sqrt{1+4(K_1-K_2)}\right)\\
\gamma &= 1+\sqrt{1+4K_1} = 1+\frac{2}{a}i
\end{aligned}$$

transitional layer (R<1% - A>99%)

(equivalent to a blow-off plasma)

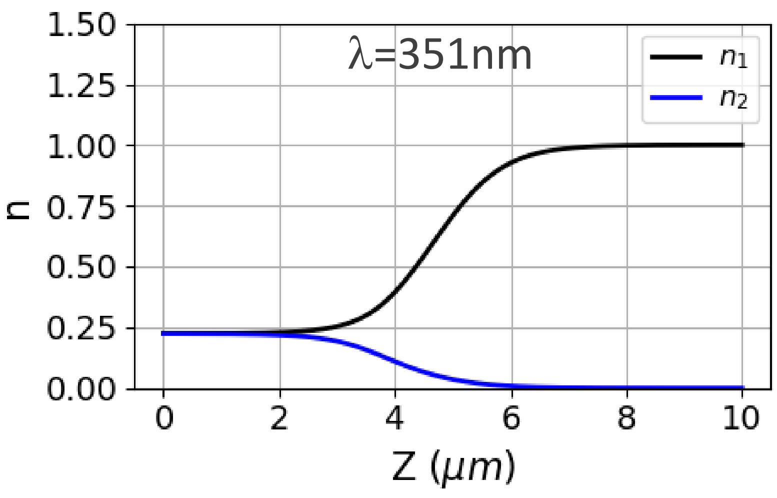

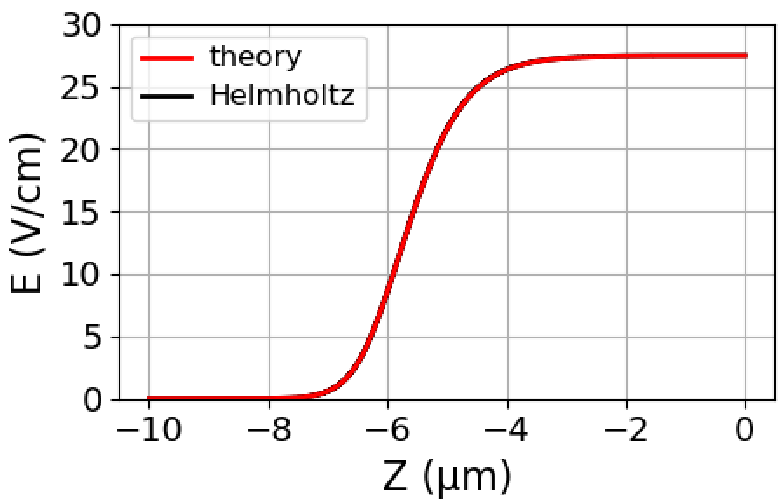

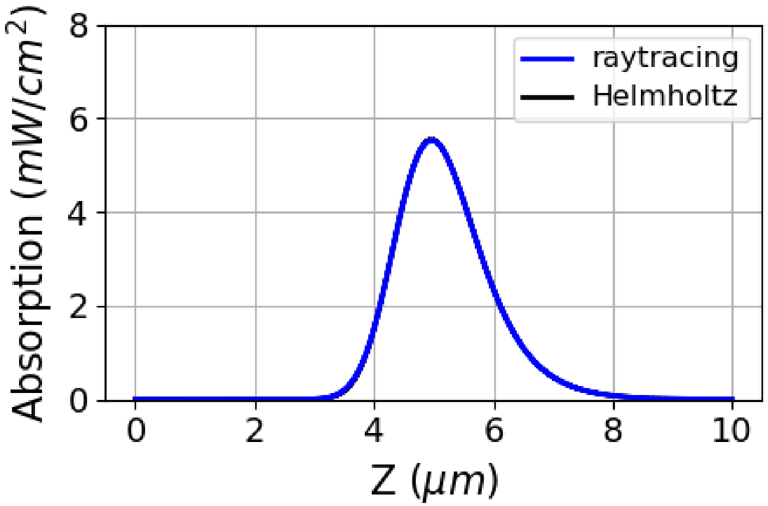

Differences appear when increasing the spatial gradient length

transitional layer (R=56.7%)
(equivalent to a sharp interface)

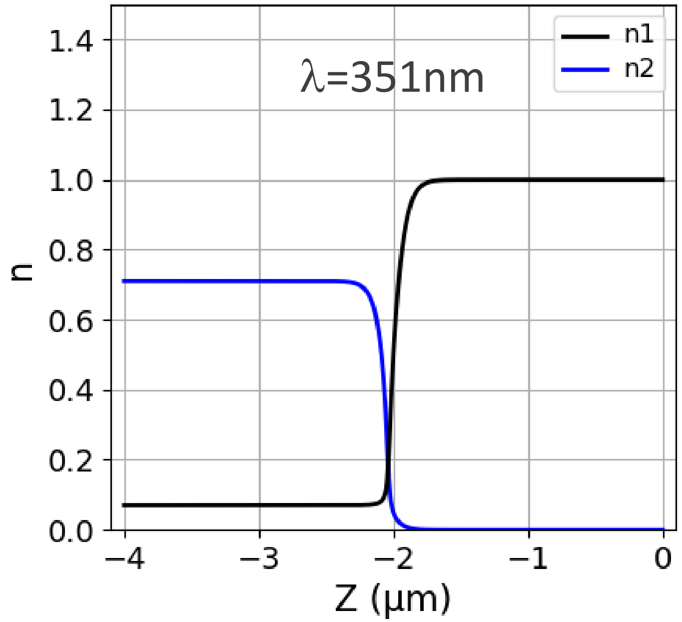

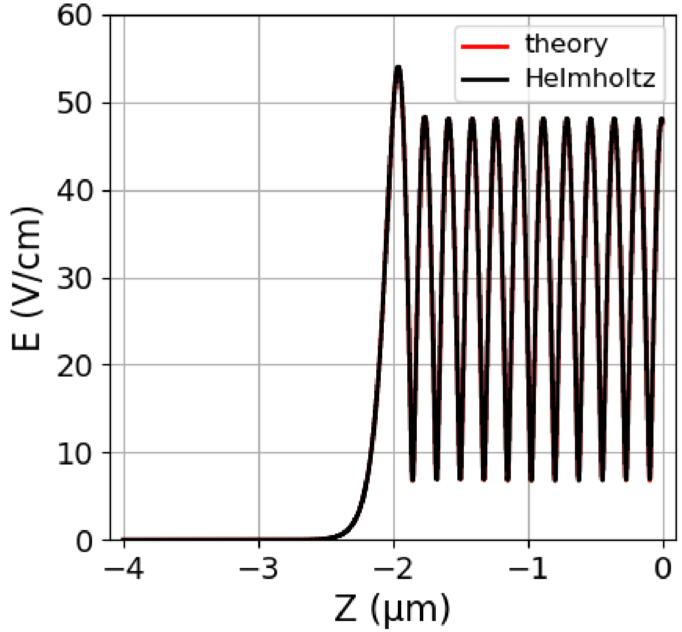

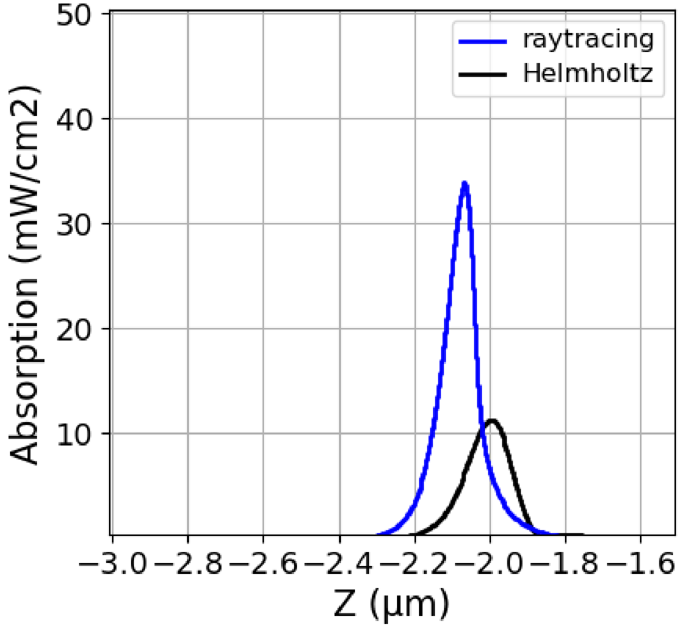

The raytracing model does not reproduce the correct energy deposition profile and the reflectivity due to the sharp interface

Optical properties for solid and plasma domain

Palik experimental data for solid domain

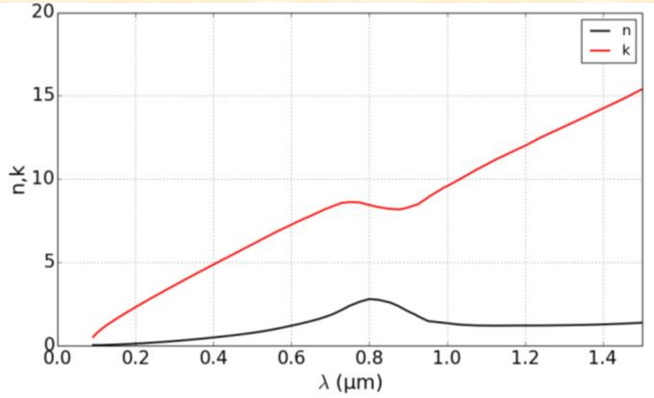

plasma domain : general formula (Atzneni, Decoster, …)

$$\varepsilon(\omega) = (n_1 - in_2)^2 = 1 - \frac{n_e}{n_c} - i\frac{n_e}{n_c}\frac{\nu_{ei}}{\omega}$$

$$v_{ei} = \frac{4}{3}\sqrt{2\pi}\frac{n_e Z e^4 ln\Lambda_{ei}}{(4\pi\varepsilon_0)^2\sqrt{m_e}(k_b T)^{3/2}}$$

$$\frac{n_e}{n_c} \ll 1 \quad \Rightarrow \quad n = \sqrt{1 - \frac{n_e}{n_c}} \quad and \quad k = \frac{1}{2n}\frac{n_e}{n_c}\frac{\tilde{\nu}_{ei}}{\omega}$$

Optical properties from solid to plasma domain
P. Combis, G.Faussurier, C. Blancard and A.Decoster work

WDM and plasma domain : Lorentz model (Landau-Lifshitz physical kinetics)

$$\sigma(\omega) = -\frac{4\pi e^2}{3m_e}\int_0^{+\infty}\frac{1}{\upsilon_{ei}(v)+i\omega}\frac{\partial f_D}{\partial v}v^3dv \quad \text{with } \upsilon_{ei}(v)=G_p v^p$$

- G_p determined by using static conductivity σ_0*
- *p is fixed by an arbitrary spline function (-3<p<1)*

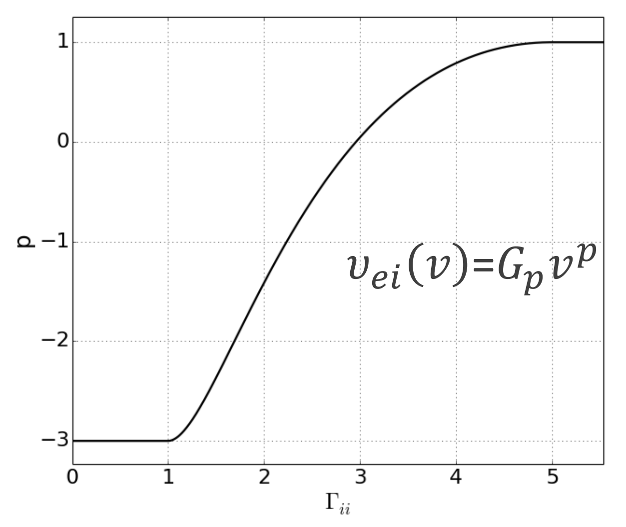

- *p=0 : Drude model*
- *p=-3 and $\upsilon_{ei} \ll \omega$: plasma model*

$$n = \sqrt{1-\frac{n_e}{n_c}} \quad \text{and } k=\frac{1}{2n}\frac{n_e}{n_c}\frac{\tilde{\upsilon}_{ei}}{\omega}$$

*G. Faussurier et al, 'Electrical and thermal conductivities in dense plasma', PoP 21 (2014)
*G. Faussurier et al, 'Electronic transport coefficients in plasmas using …', PoP 24 (2017)

Outline

- Laser-matter interaction models for one-dimensional codes
  - Numerical methods
  - Optical properties
- **Experiments for ablation pressure characterization**
  - Direct interaction in vacuum
  - Confinement regime
- 2D effects
- Laser ablation experiments on ELFIE
- LAser Shock Adherence Test

Experimental characterization of laser-matter interaction: development of the GCLT laser platform (E. Lescoute & A. Sollier)

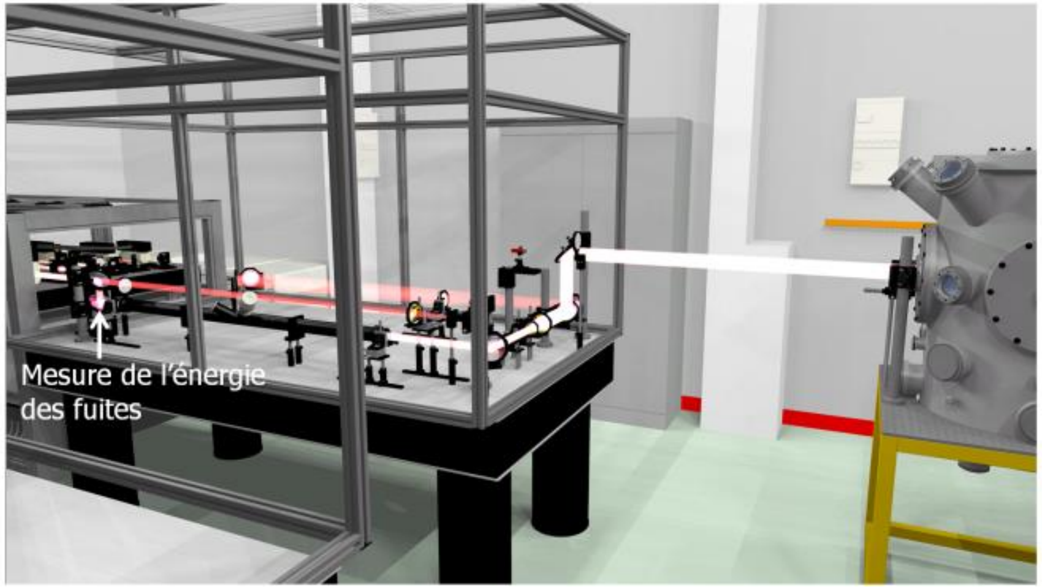

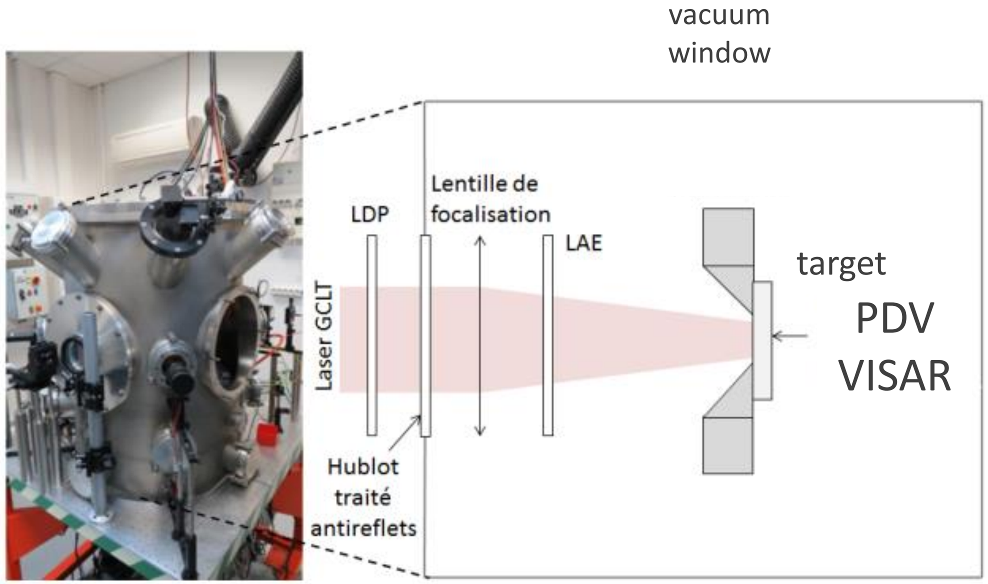

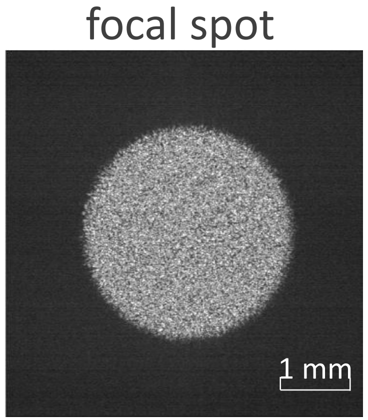

- Laser Nd:YAG @ 1053nm ; E<40J ; 1 shot – 2 mn
- Temporal arbitrary shape τ = 5-100 ns
- Uniform focal spot (Diffractive Optics Element) : 0.5 mm → 5 mm
- Rear surface velocity measurements (PDV, VISAR)

Direct Laser-matter interaction characterization based on Free Surface Velocity measurements (1053nm ; 10-40ns ; 10-400 GW/cm²)

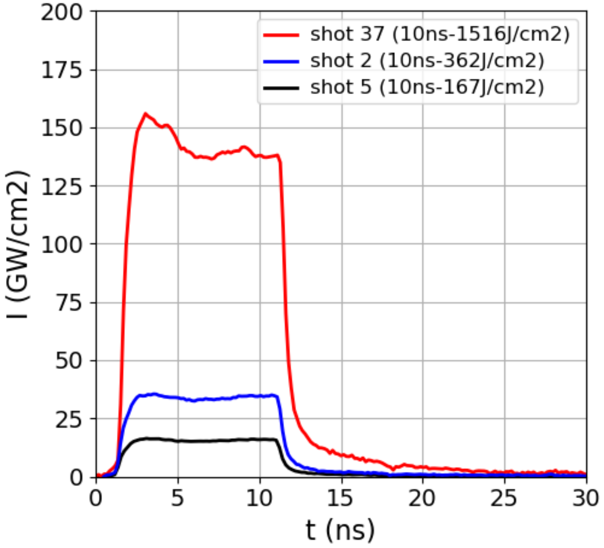

vacuum experiments

100µm - Al

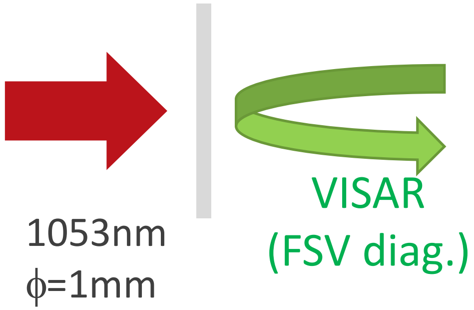

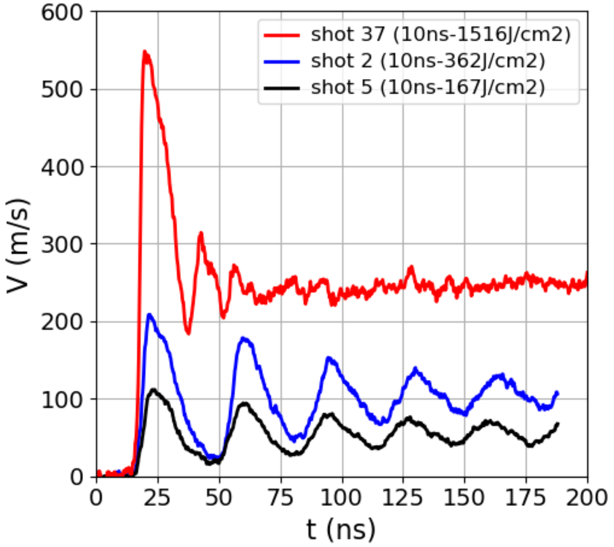

Numerical study with the Esther code (Helmholtz equation)

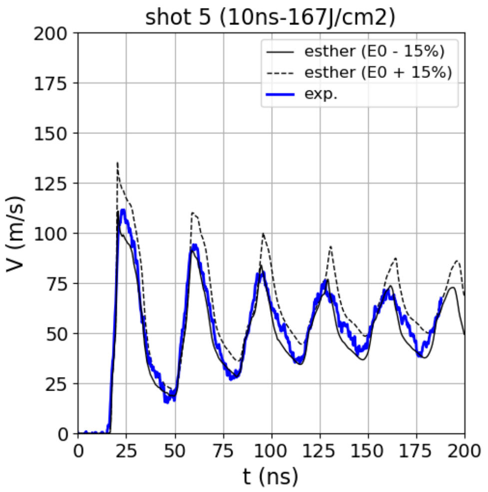

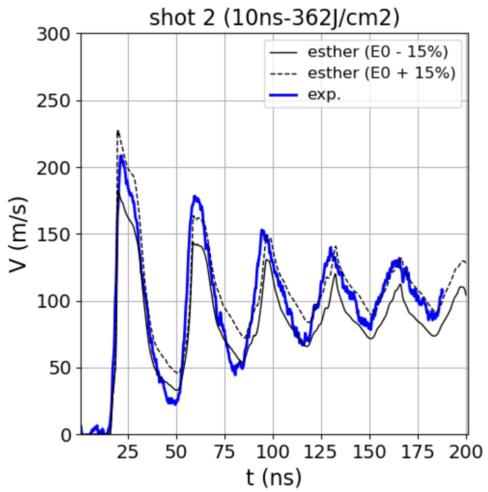

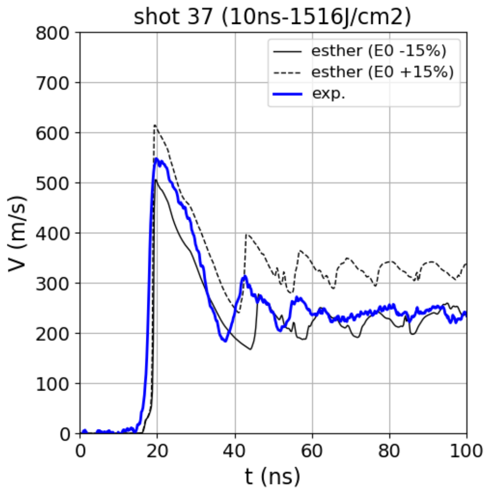

** S. Bardy et al, JOLT 124 (2020)*

** M. Scius-Bertrand et al, JPhysD (2021)*

Raytracing method versus Helmholtz equation resolution for direct laser-matter interaction

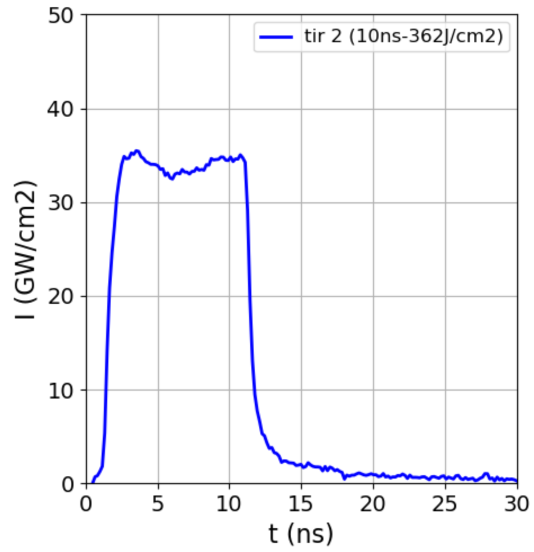

vacuum experiments

100µm - Al

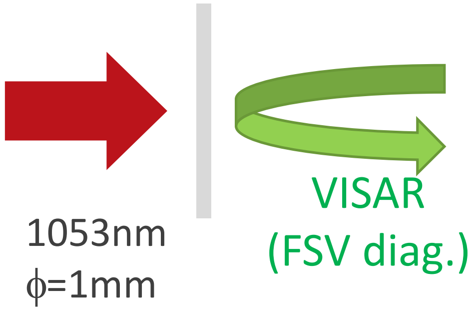

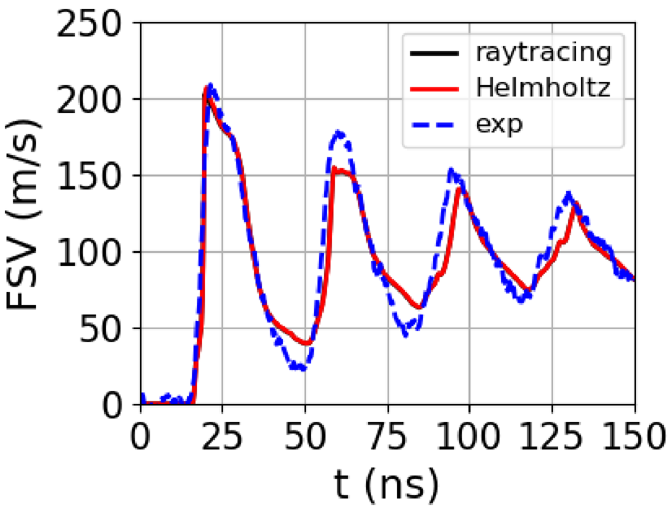

No difference in numerical VISAR

Temporal laser energy deposition evolution

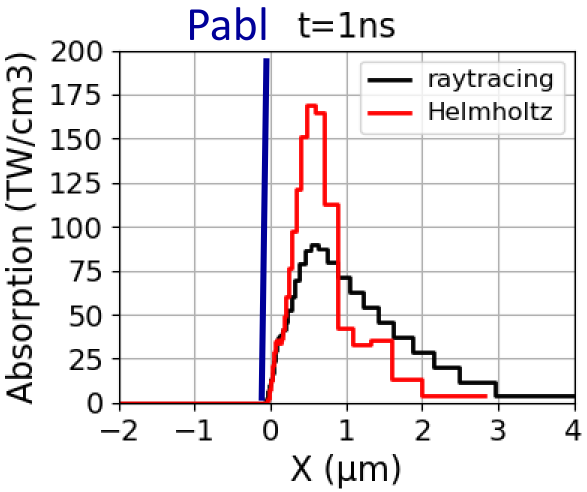

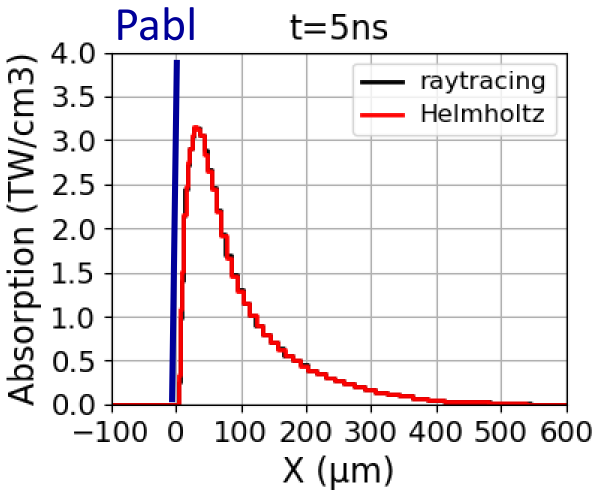

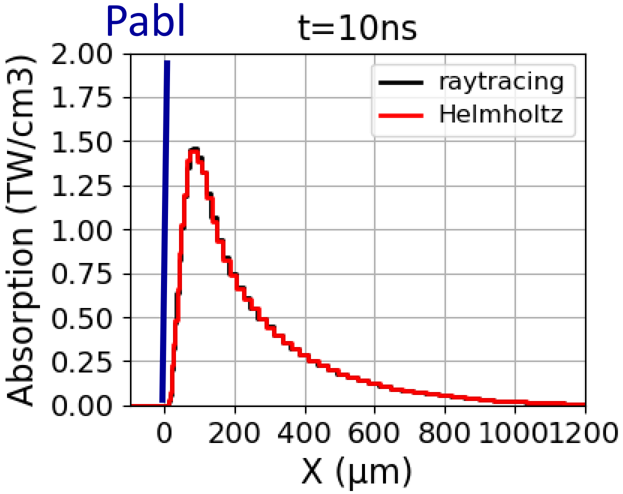

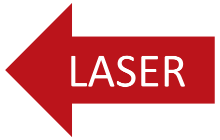

Ablation pressure calculation by using numerical simulations

"The ablation pressure is calculated in order to reproduce the shock wave induced by the laser-matter interaction"

$$P_{abl}(t) = P(t, X(V = 0))$$

** M. Scius-Bertrand et al, JPhysD (2021)*

Numerical simulation with the laser-matter interaction model
100µm aluminum – 10 ns –360 J/cm²

Numerical simulation with the calculated ablation pressure

Numerical ablation pressure

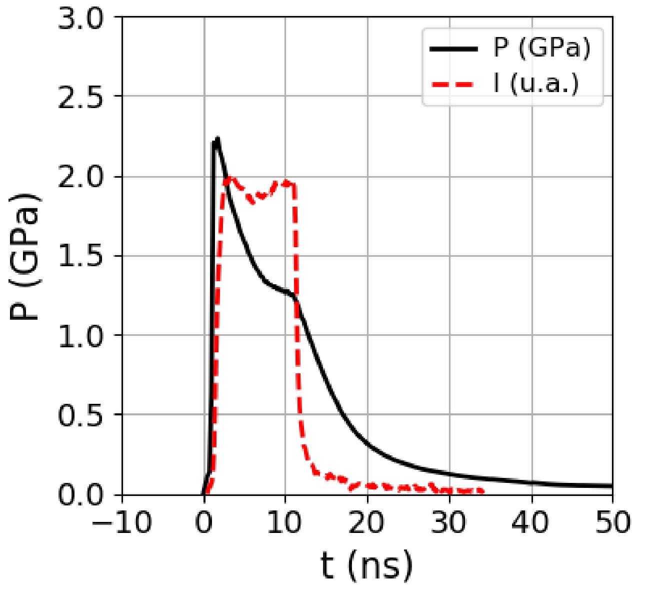

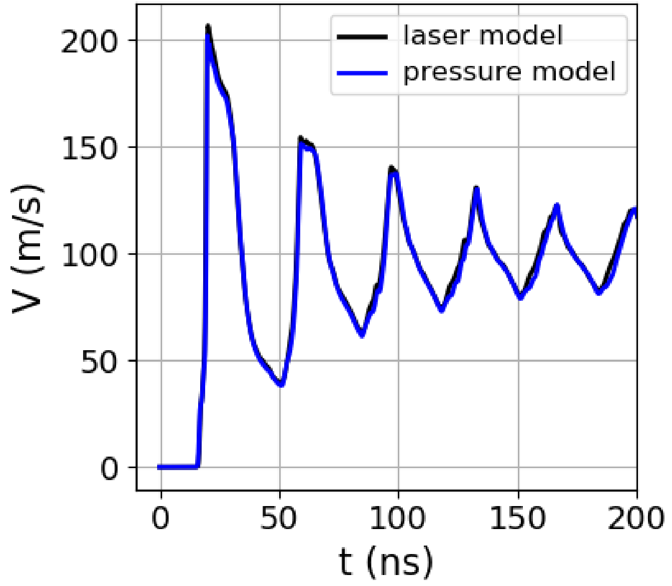

Analytical fits based on ESTHER calculations : input for MONARQUE & COMPOCHOC FUI projects

Goal : input for 2D/3D codes, optimization, etc .

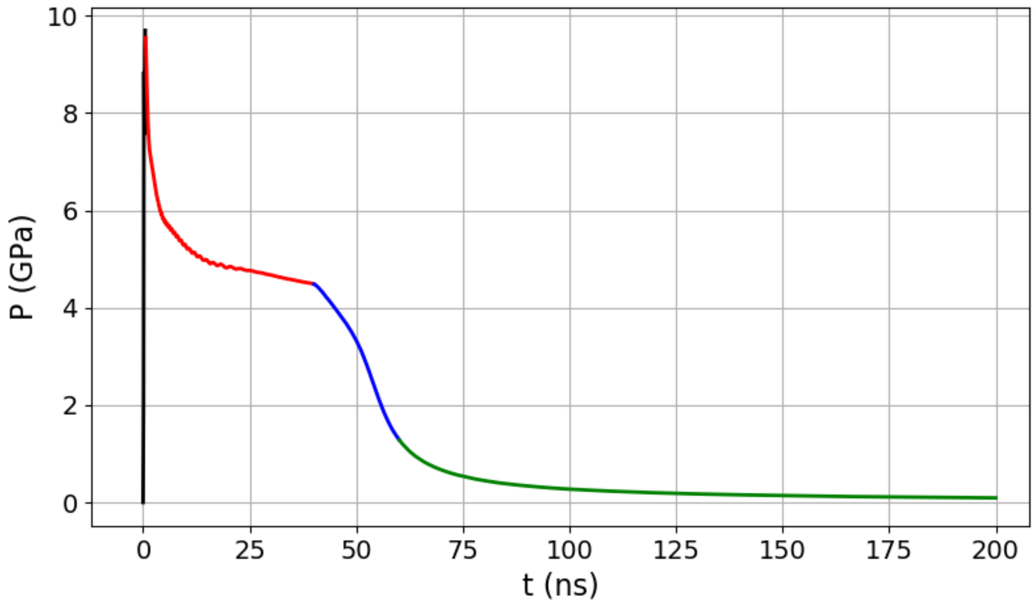

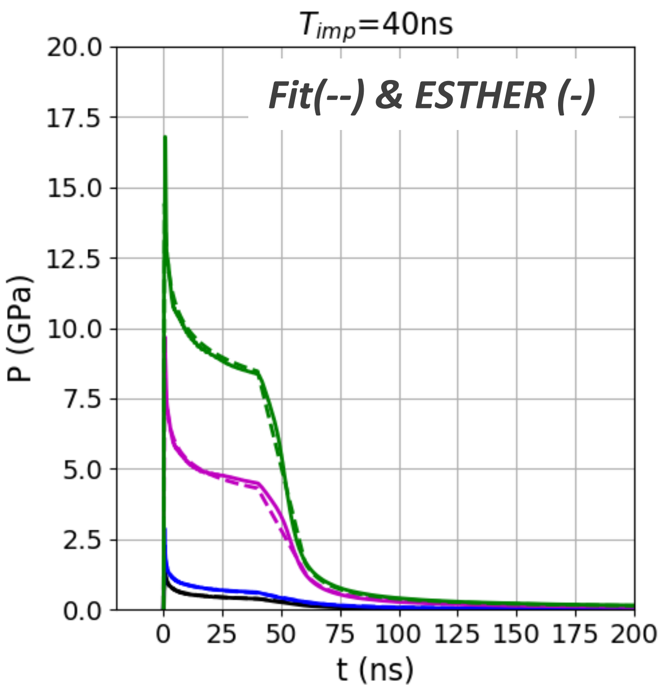

$$t \leq T_0 \ : P(t) = P_{max}\left(\frac{t}{T_0}\right)$$

$$T_0 \leq t \leq T_{imp} : P(t) = P_{max}\left(\frac{T_0}{t}\right)^p$$

$$T_i \leq t : P(t) = P_i\left(\frac{T_i - T_i\delta}{t - T_i\delta}\right)^n$$

$\boldsymbol{All\ the\ parameters\ depend\ on\ Timp\ \ (ns) and\ I(GW/cm^2)}$

Laser-matter interaction platform in confinement regime in GCLT Plaform and Hephaïstos (Y. Rouchausse & L. Berthe)

Hephaïstos laser platform (PIMM – ENSAM)

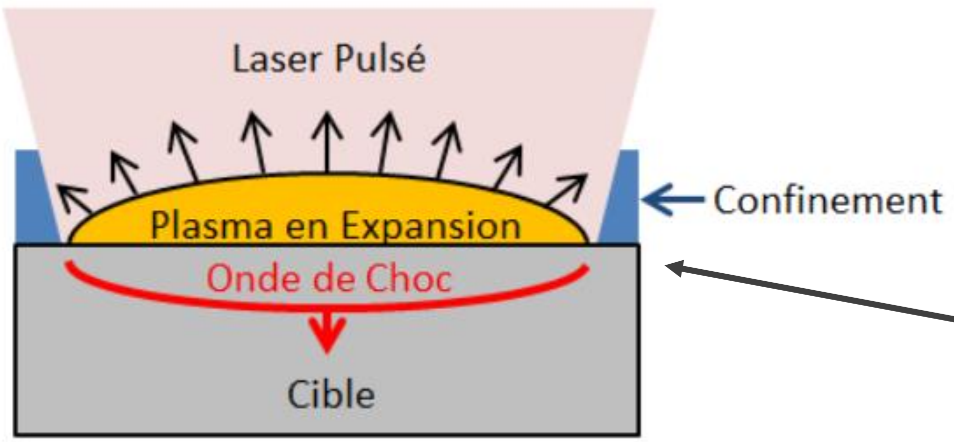

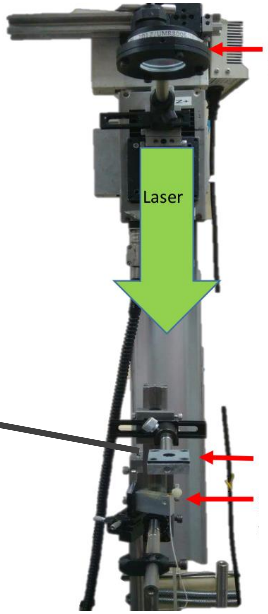

Lens + DOE

target

PDV/VISAR

532 nm
2x7 J
7ns

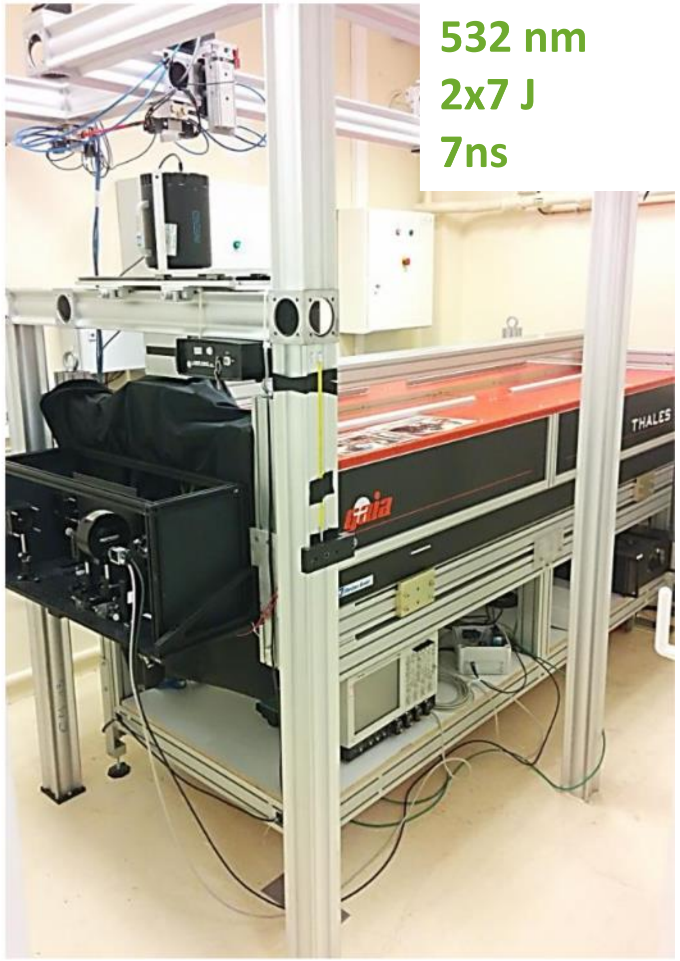

- The confinement material increases the induced pressure (x10)
- Laser configuration for industrial processes (LASAT, LSP)
- Intensity below the laser breakdown (between 5 and 10 GW/cm^2)
- Maximum ablation pressure ≈ 10 GPa

Laser-matter characterization in confinement regime : same approach to finally obtain numerical ablation pressure fits & 532/1053m

532nm-7 ns
Gaussian pulse
ϕ= 4mm

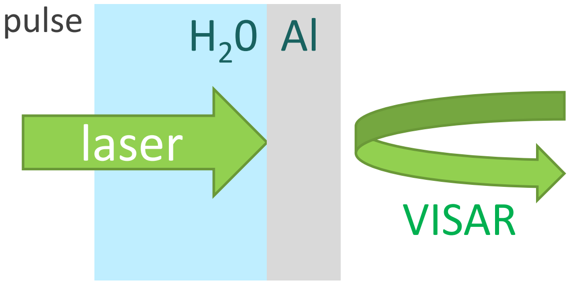

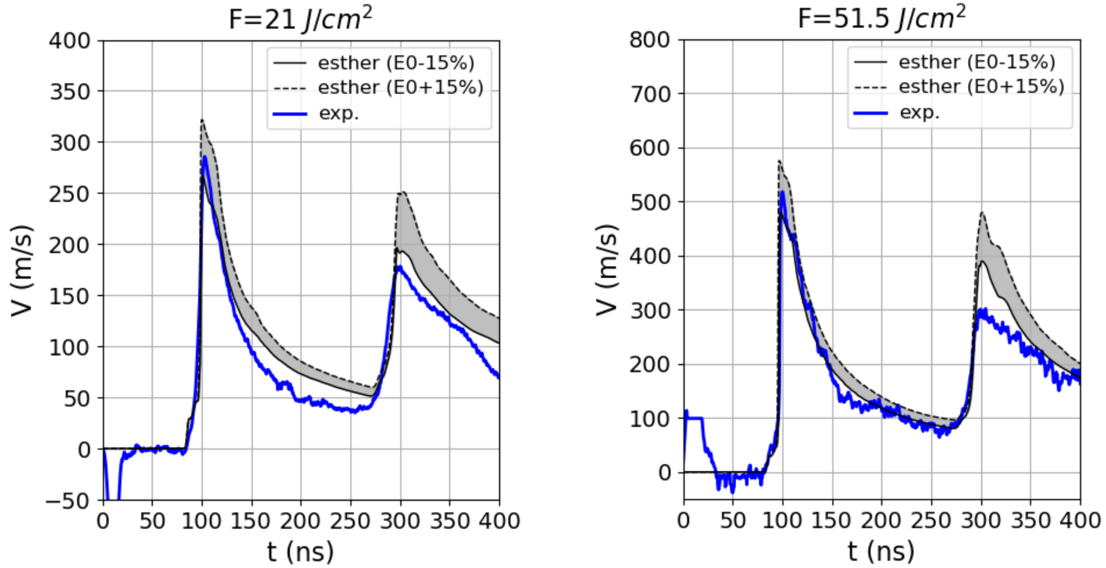

Numerical study with the Esther code (Helmholtz equation)

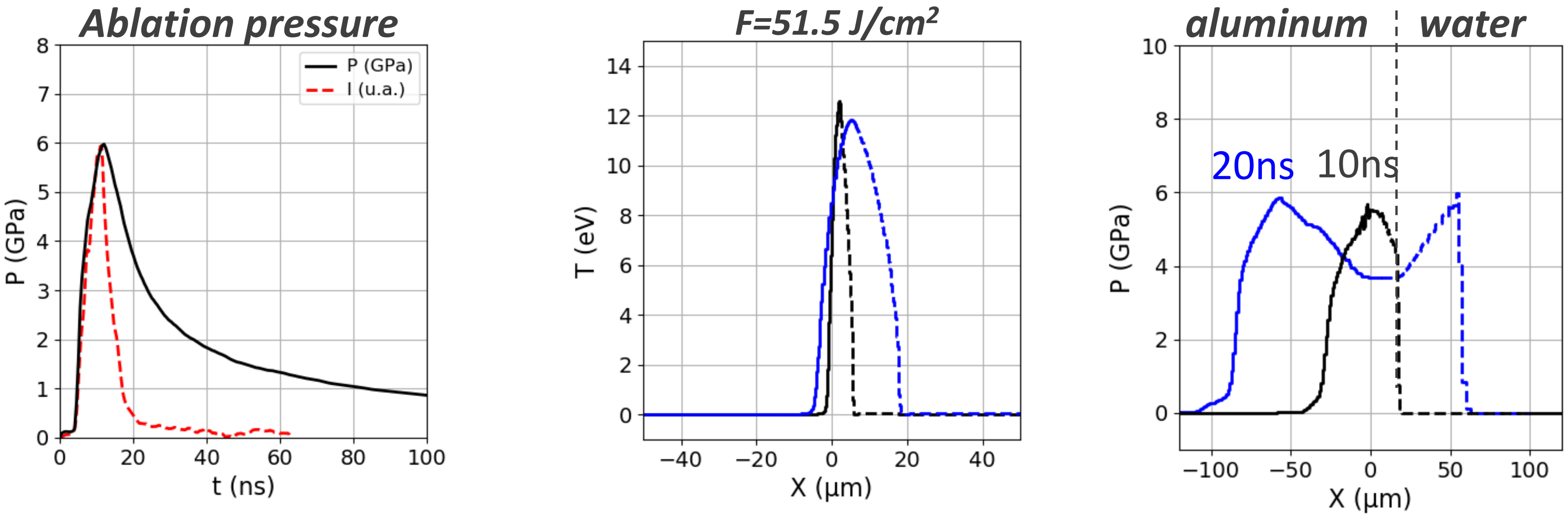

Outline

- **Laser-matter interaction models for one-dimensional codes**
  - Numerical methods
  - Optical properties
- **Experiments for ablation pressure characterization**
  - Direct interaction in vacuum
  - Confinement regime
- **2D effects**
- **Laser ablation experiments on ELFIE**
- **LAser Shock Adherence Test**

2D effects study: direct illumination on GCLT platform (still in progress)

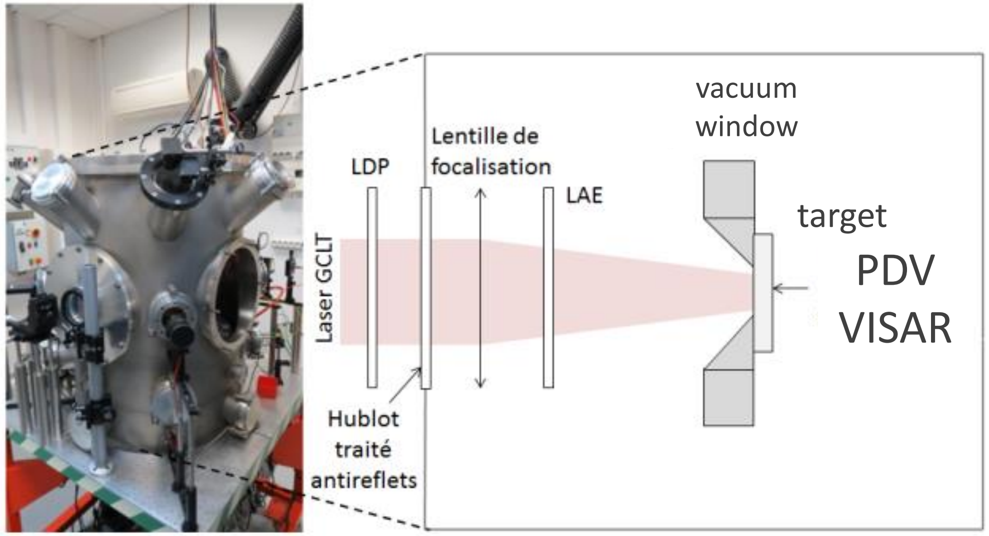

focal spot measurements

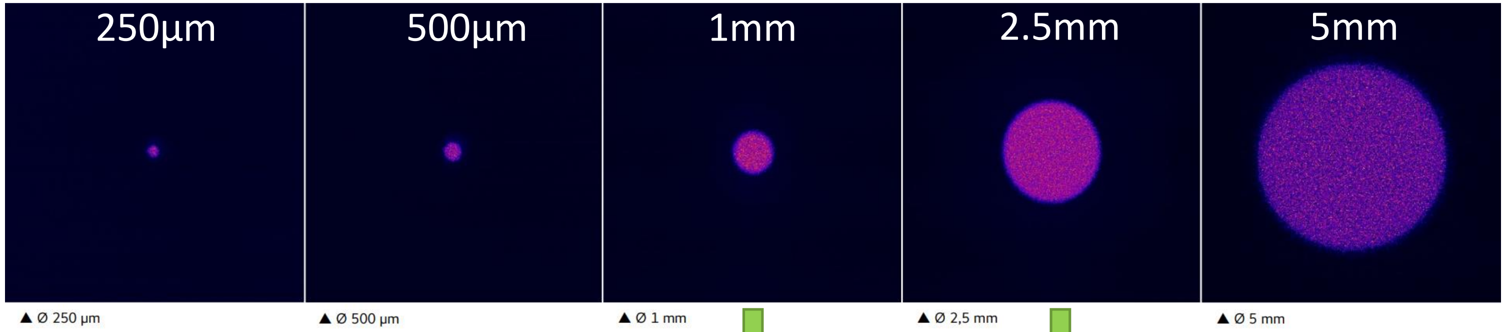

38 GW/cm²

Al-100 µm
10 ns

36 GW/cm²

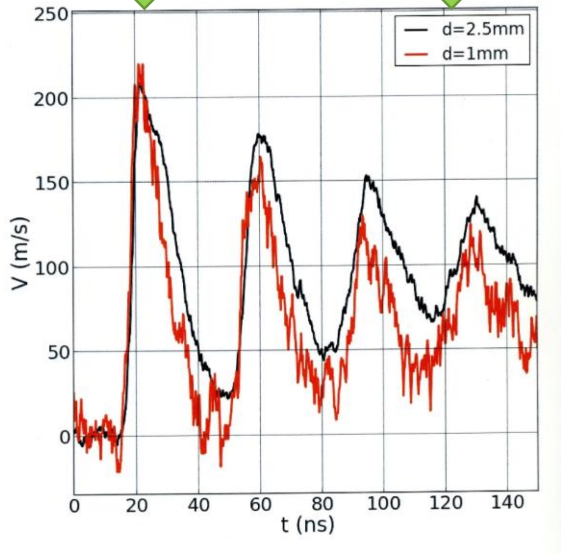

The release is shorter when the focal spot is smaller

(work to continue with different focal spot an pulse durations)

2D effects study: confined regime (Hephaïstos plaform) – A. Rondepierre thesis (ANR ForgeLaser)

"Beam size dependency of a laser-induced plasma in confined regime …", A. Rondepierre et al, JOLT 135 (2021)

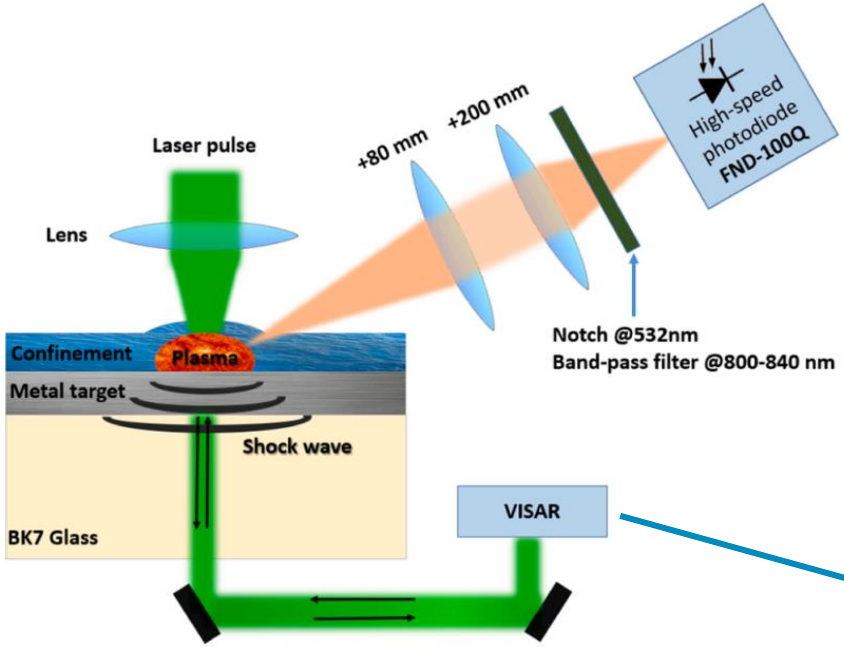

Effect on temperature

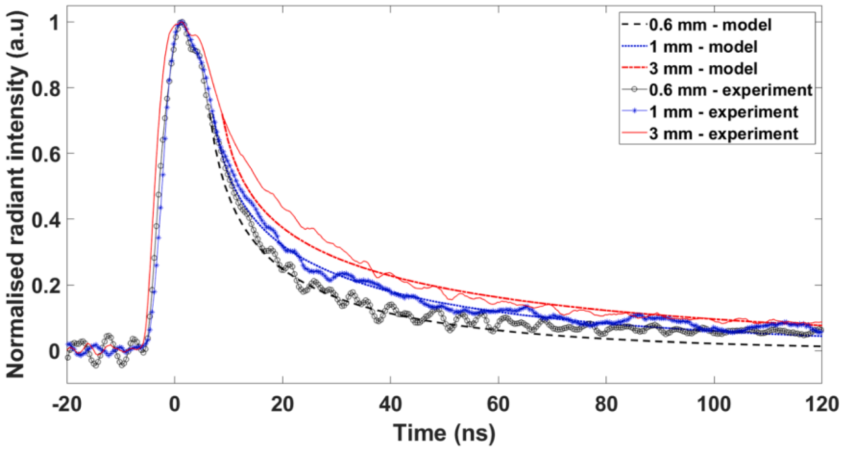

Effect on the induced shock wave

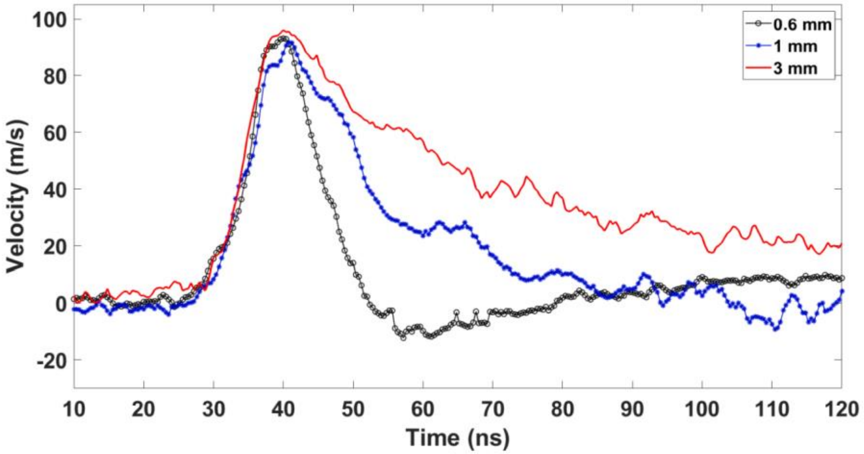

2D effects study: confined regime

"Beam size dependency of a laser-induced plasma in confined regime …", A. Rondepierre et al, JOLT 135 (2021)

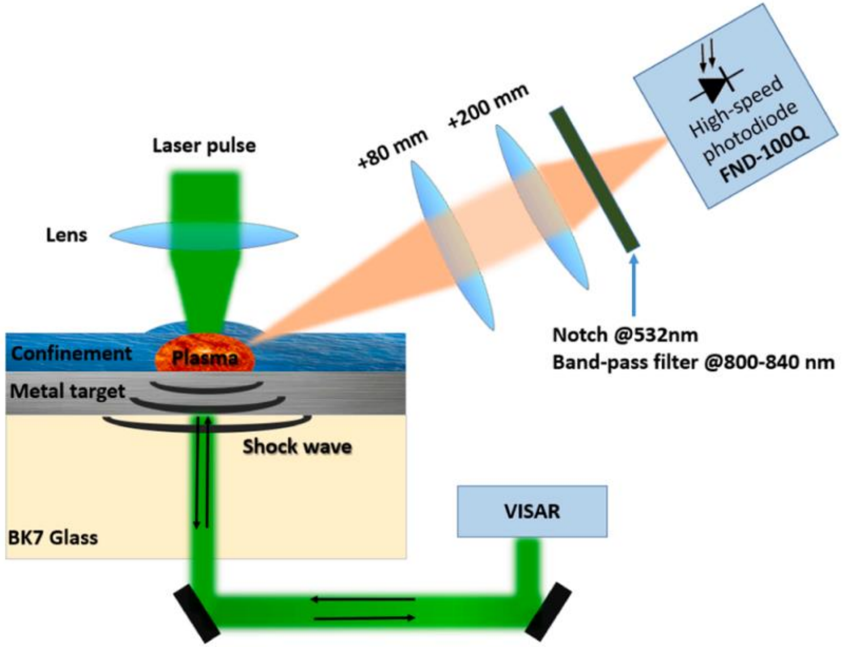

1D/2D ablation pressure calculations

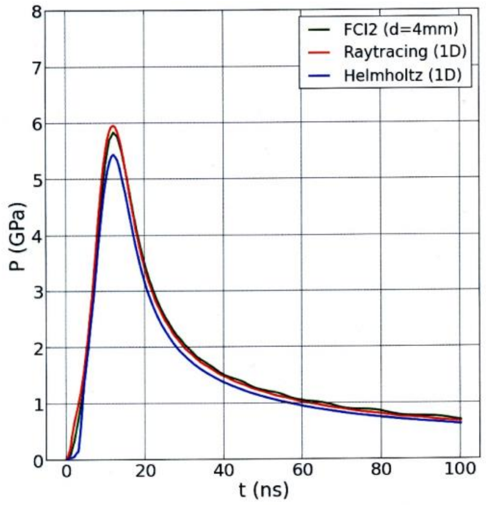

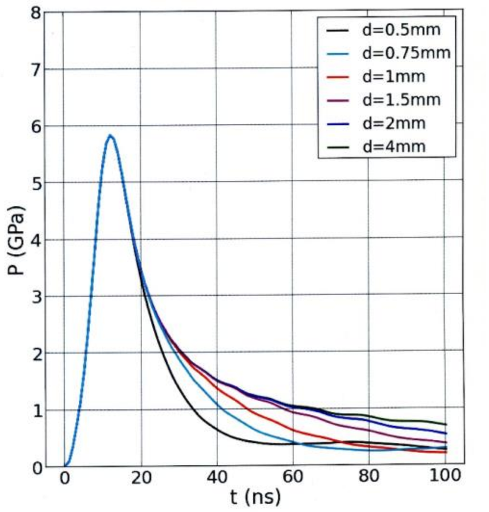

Spatial applications using laser ablation : 3 years ELFIE proposal

LULI (S. Baton, E. Brambrink) – PIMM (L. Berthe) – CEA/DAM (J.M. Chevalier, C. Rousseaux, L. Videau)
CNES (C. Bonnal, F. Masson) – CEMEF (S. Boyer) – ENSMA (M. Boustie) – C. Phipps

Removing or reorbiting debris

Laser propulsion *

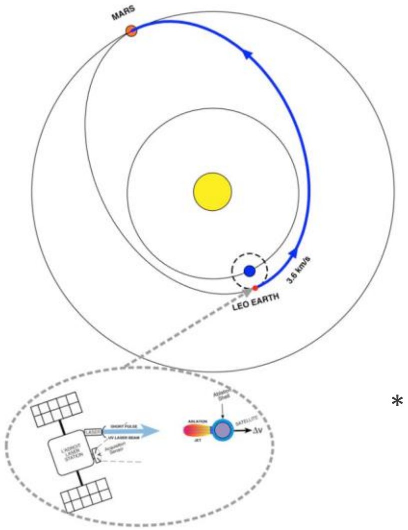

* see S. Boyer talk

C. Phipps, et al., “Laser impulse coupling measurements at 400 fs and 80 ps using the LULI facility at 1057 nm wavelength”, JAP 122 (2017)
C. Phipps, “Transfers from Earth to LEO and LEO to interplanetary space using lasers" *Acta Astronautica,* 146 (2018)

Pendulum experiments to study laser-matter ablation process for different pulse durations (400fs – 80ps – 600ps)

Pump Laser

λ=1053 nm ; τ=400 fs, 80 ps, 600ps

E=1-10 J ; ϕ=7 mm or 5mm

Probe Laser (chirped)

λ=1053 nm ; τ=500 ps

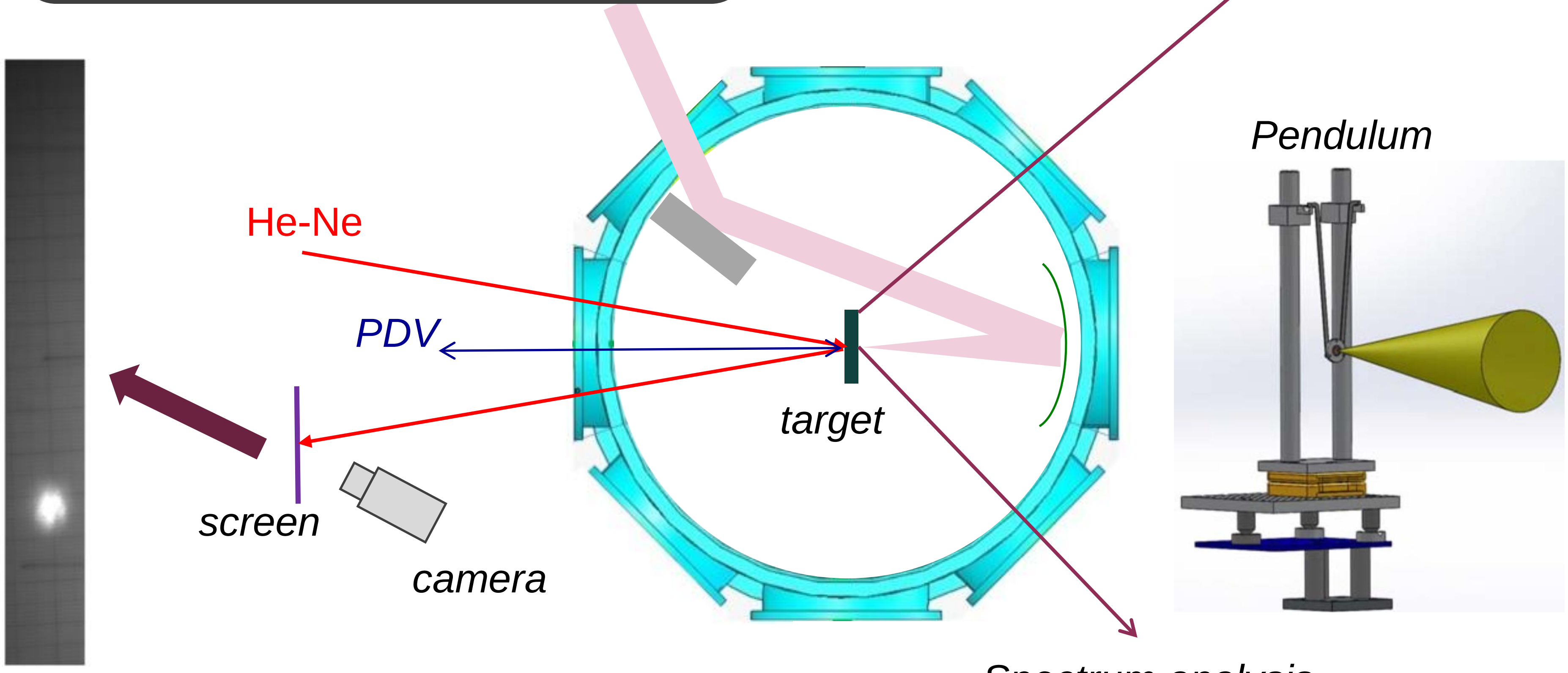

ELFIE @ LULI, Ecole Polytechnique (France)

Intermediate 80 ps pulse duration show the highest coupling coefficent

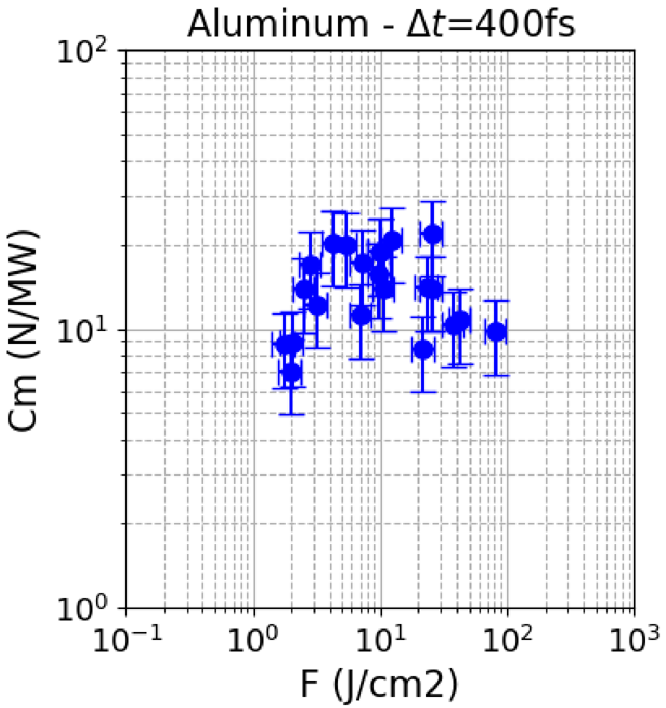

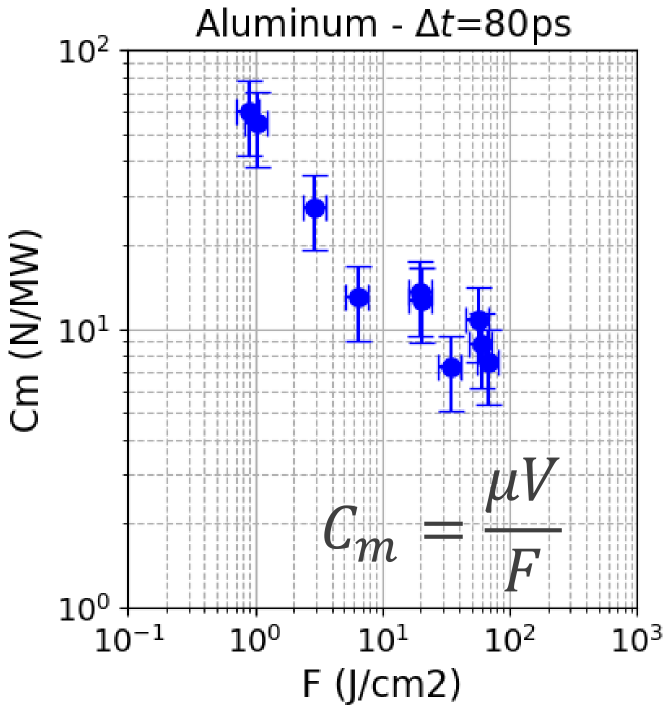

$$C_m = \frac{\mu V}{F}$$

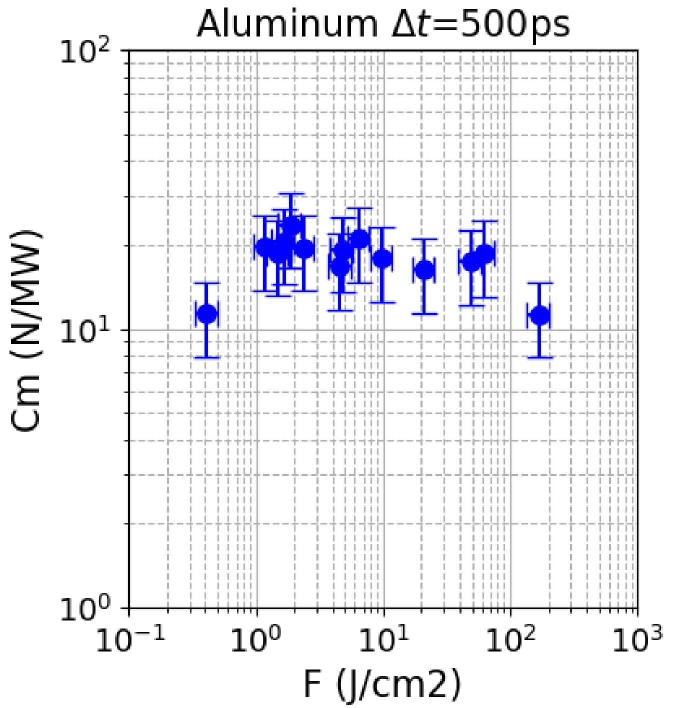

Simulations and experiments are in the same order of magnitude but differences still exist

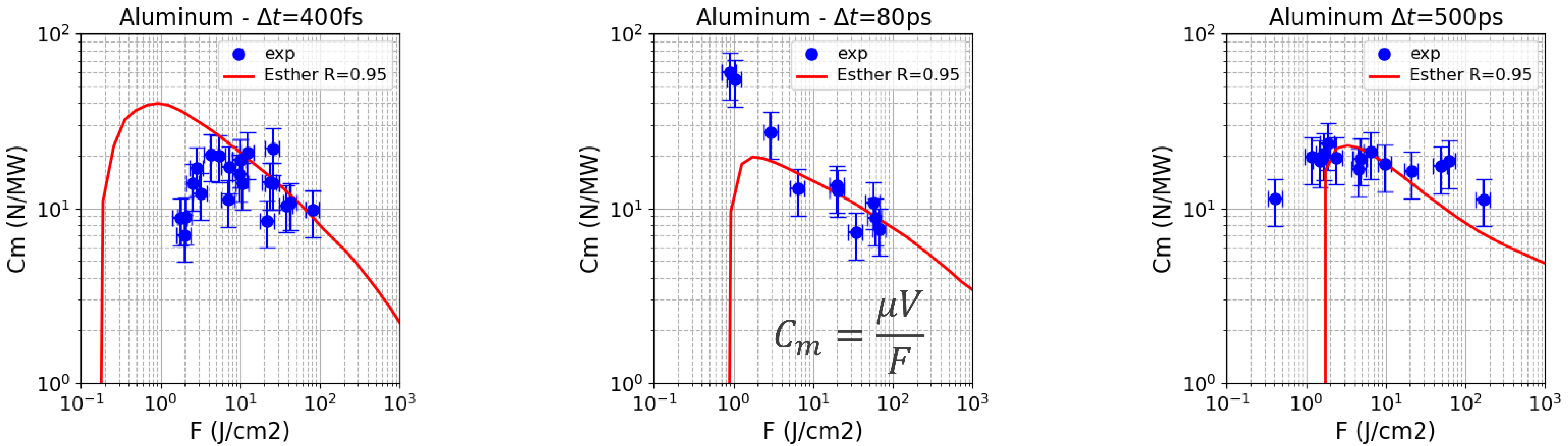

- Two temperature model needs more accurate data ?
- Ejection debris are not taken into account in our simulations ?
- Help ? ☺

Influence of the initial solid reflectivity on numerical simulations

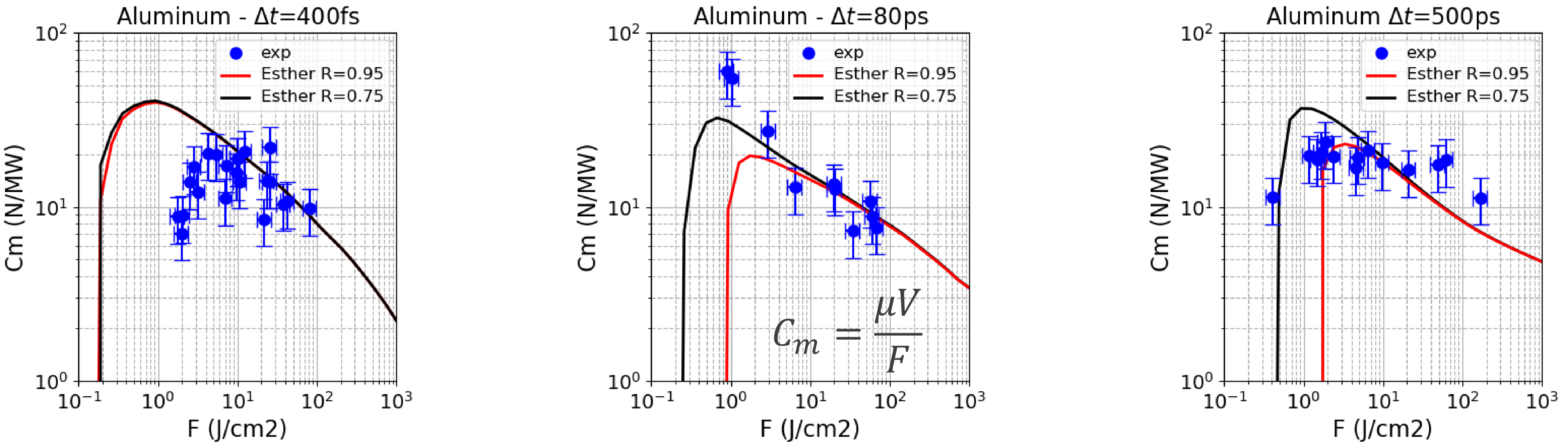

- ➢ Two temperature model needs more accurate data ?
- ➢ Ejection debris are not taken into account in our simulations ?
- ➢ Help ? ☺

- ➢ Numerical ablation threshold does not depend on the initial solid reflectivity for sub-ps pulse duration

Time-resolved reflectivity measurement for aluminum @ 80 ps

Pump Laser

λ=1053 nm

τ=400 fs -> 80 ps

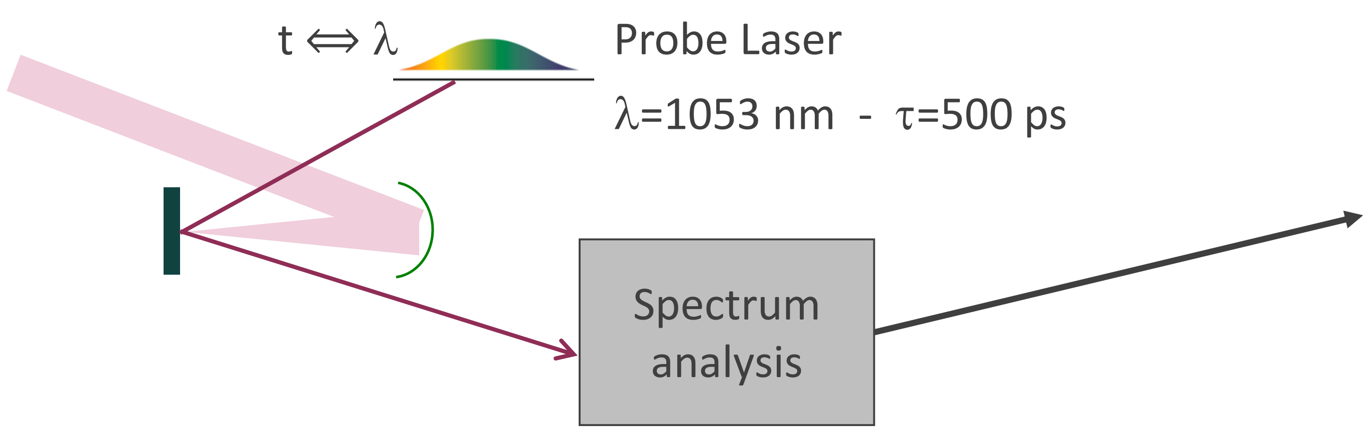

Probe Laser

λ=1053 nm - τ=500 ps

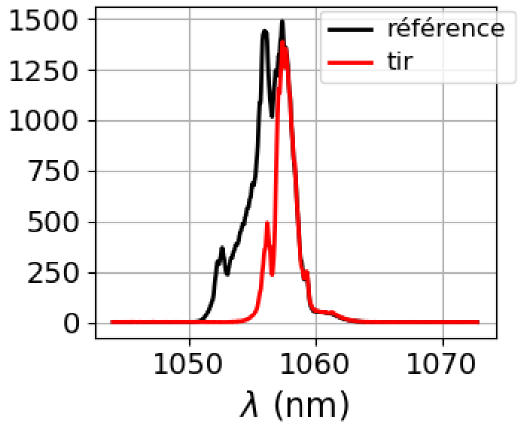

F=1.5 J/cm²

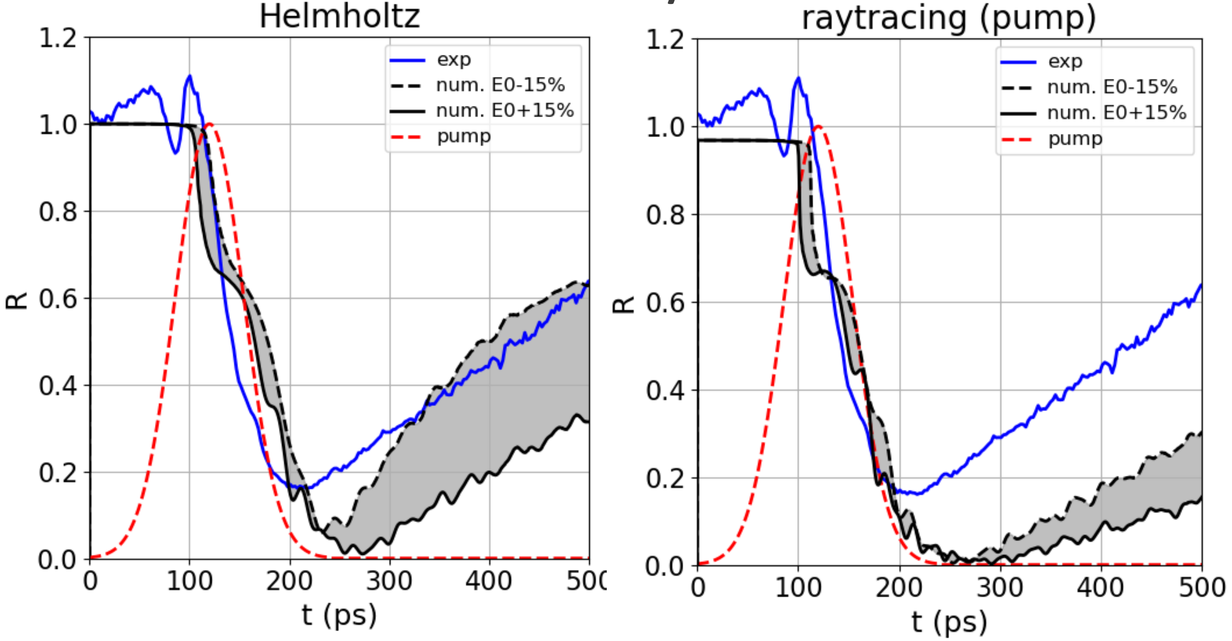

F=11 J/cm²

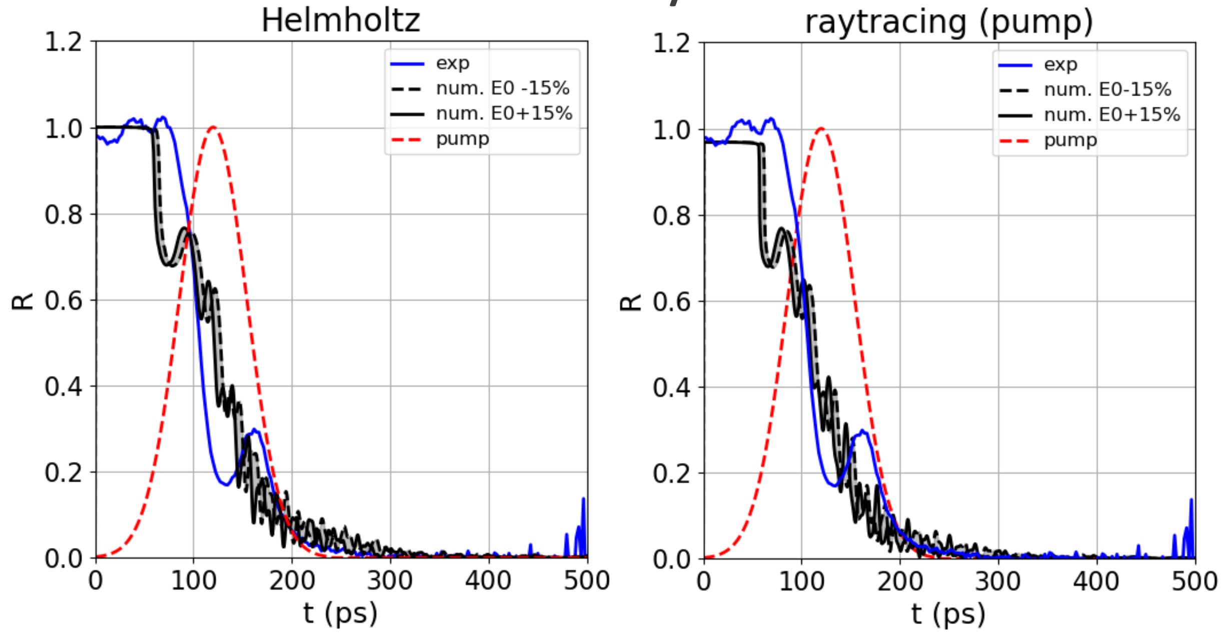

LAser Shock Adherence Test (LASAT) context

FUI projects COMPOCHOC (2016-2020) & MONARQUE (2018-2022)

Fan blades (LEAP engine)
(3D-CFRP/Ta6V4)

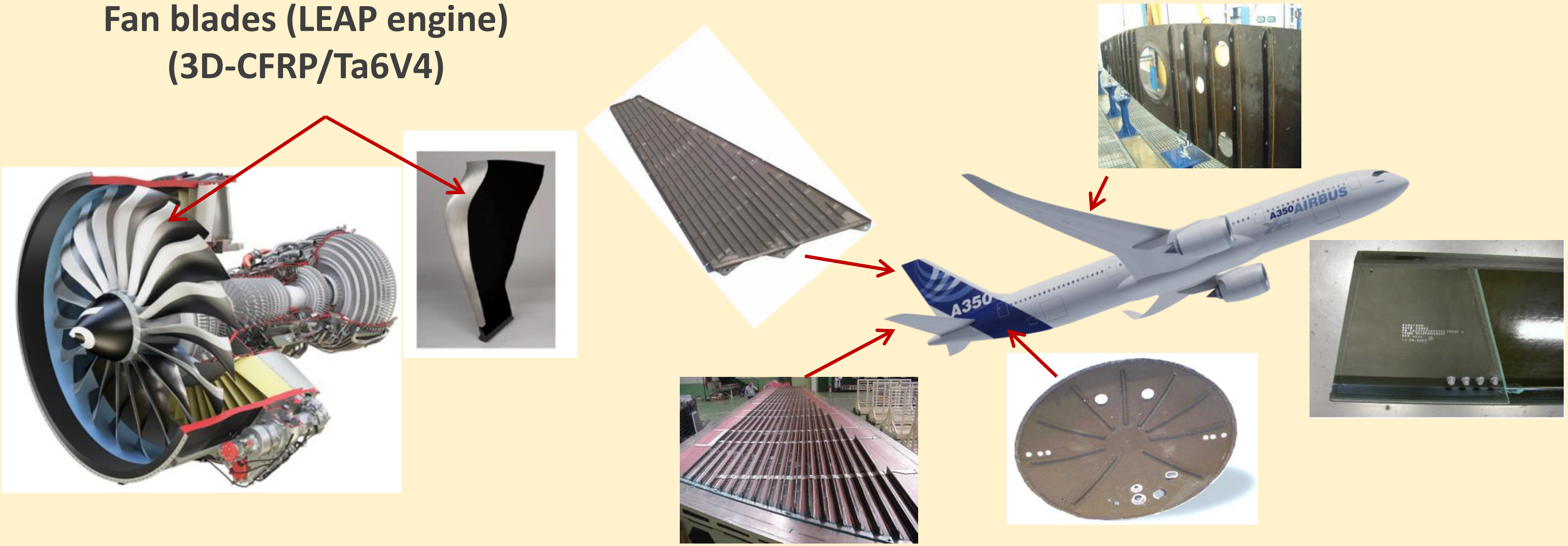

Bonded joints on the A350 aircraft
(2D-CFRP)

Goal : test and quantify the bond strength level

X-t diagram : shock wave propagation

Mono pulse configuration

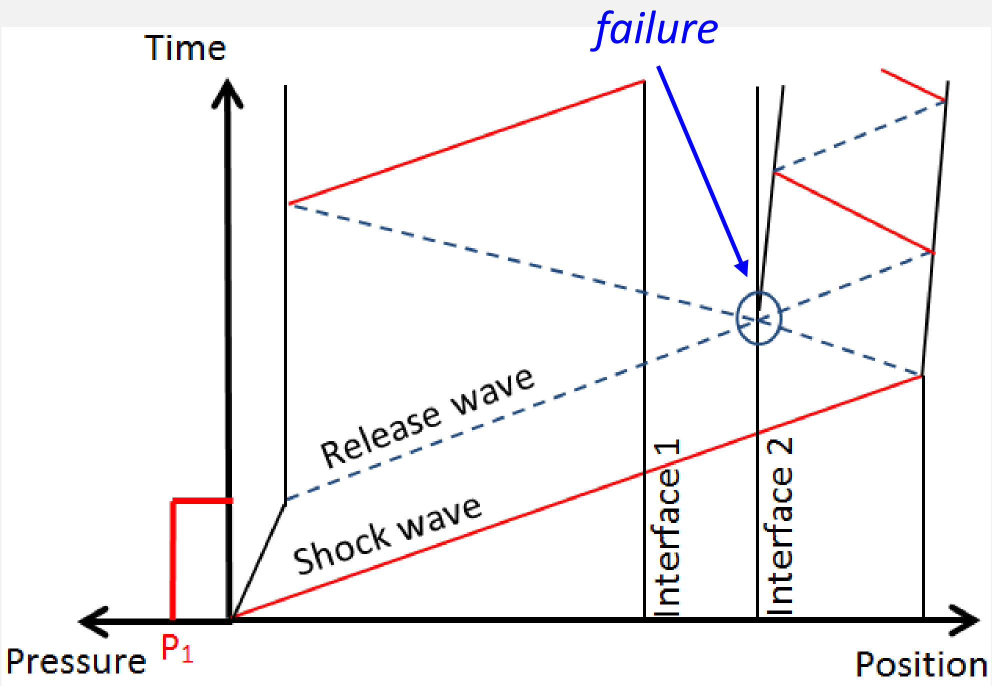

Double pulse configuration

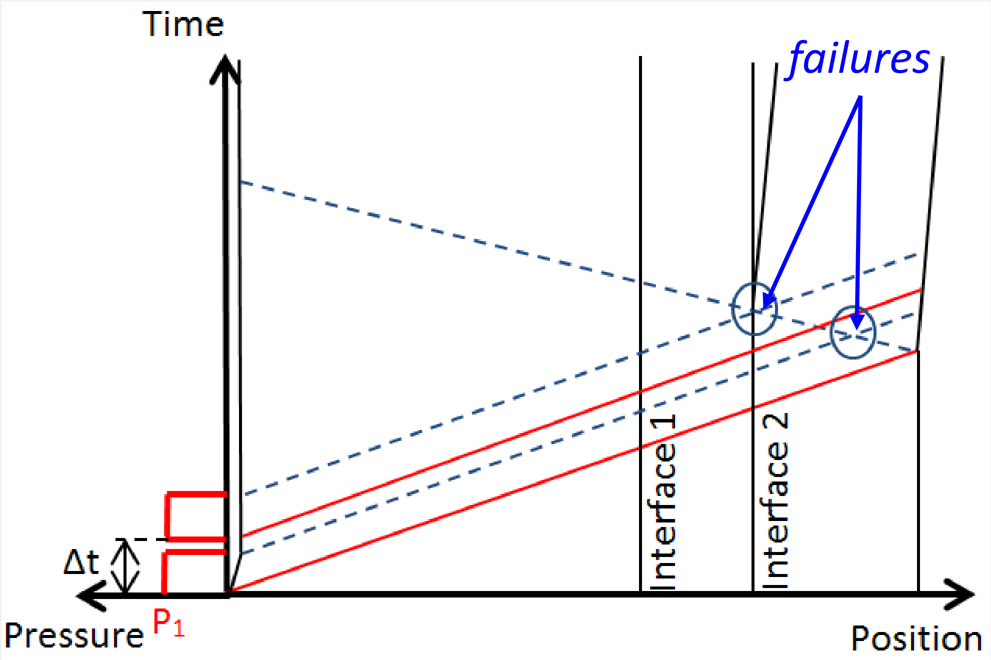

LASAT application for a Alu/epoxy/Alu assembly*

Numerical simulation validation by using VISAR measurement

X-t diagram Esther
Mono pulse GCLT shot
1053nm - 20ns – 2.9 GW/cm²

Experiment (VISAR)
Simulation (ESTHER)

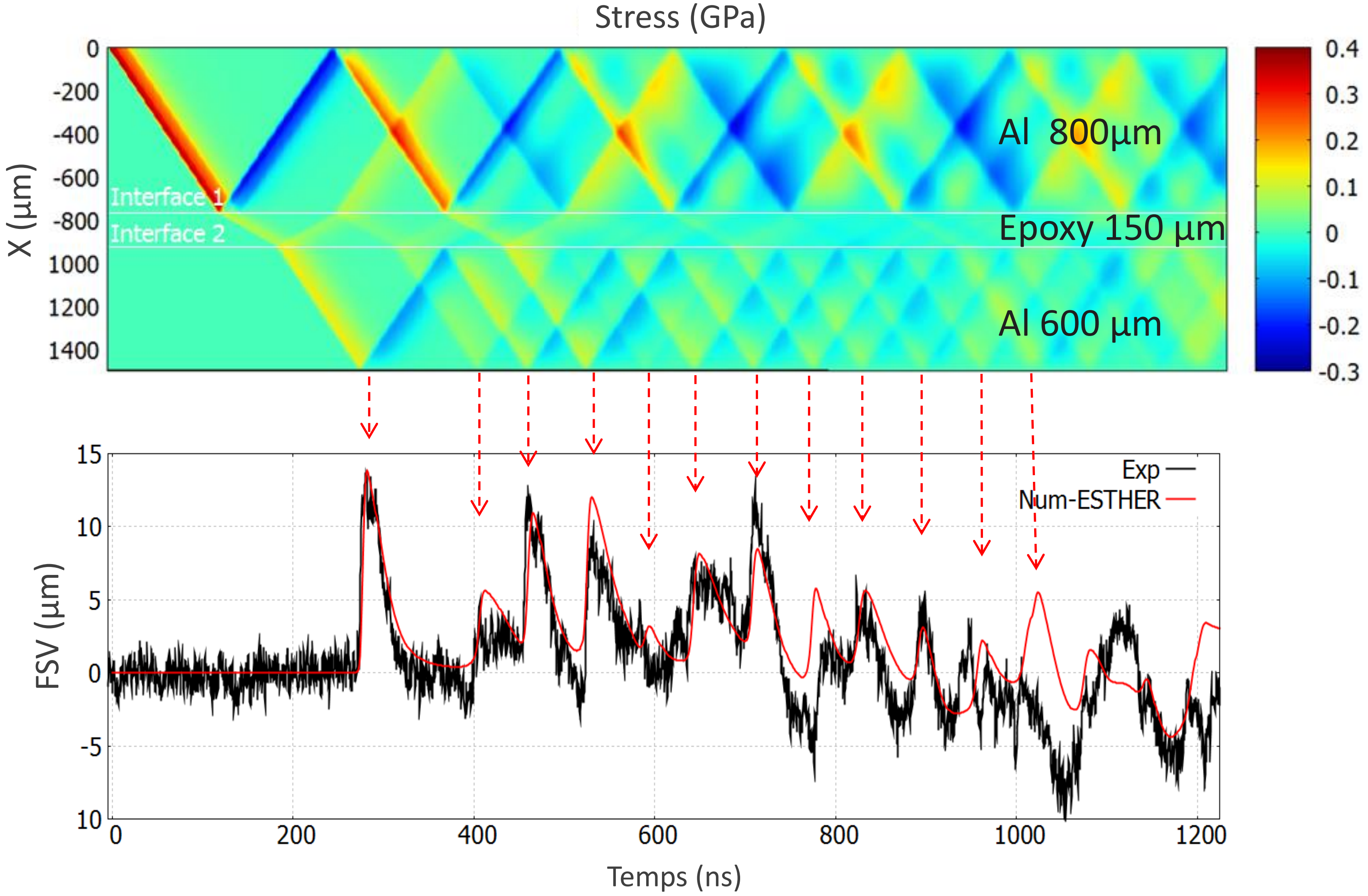

* *D. Laporte thesis CESTA (2010)*

Comparison between 1D and 2D numerical simulations

Numerical simulation validation by using VISAR measurement

X-t diagram Esther

Mono pulse GCLT shot

1053nm - 20ns – 2.9 GW/cm²

Experiment (VISAR)

Simulation 1D (ESTHER)

Simulation 2D (HESIONE)

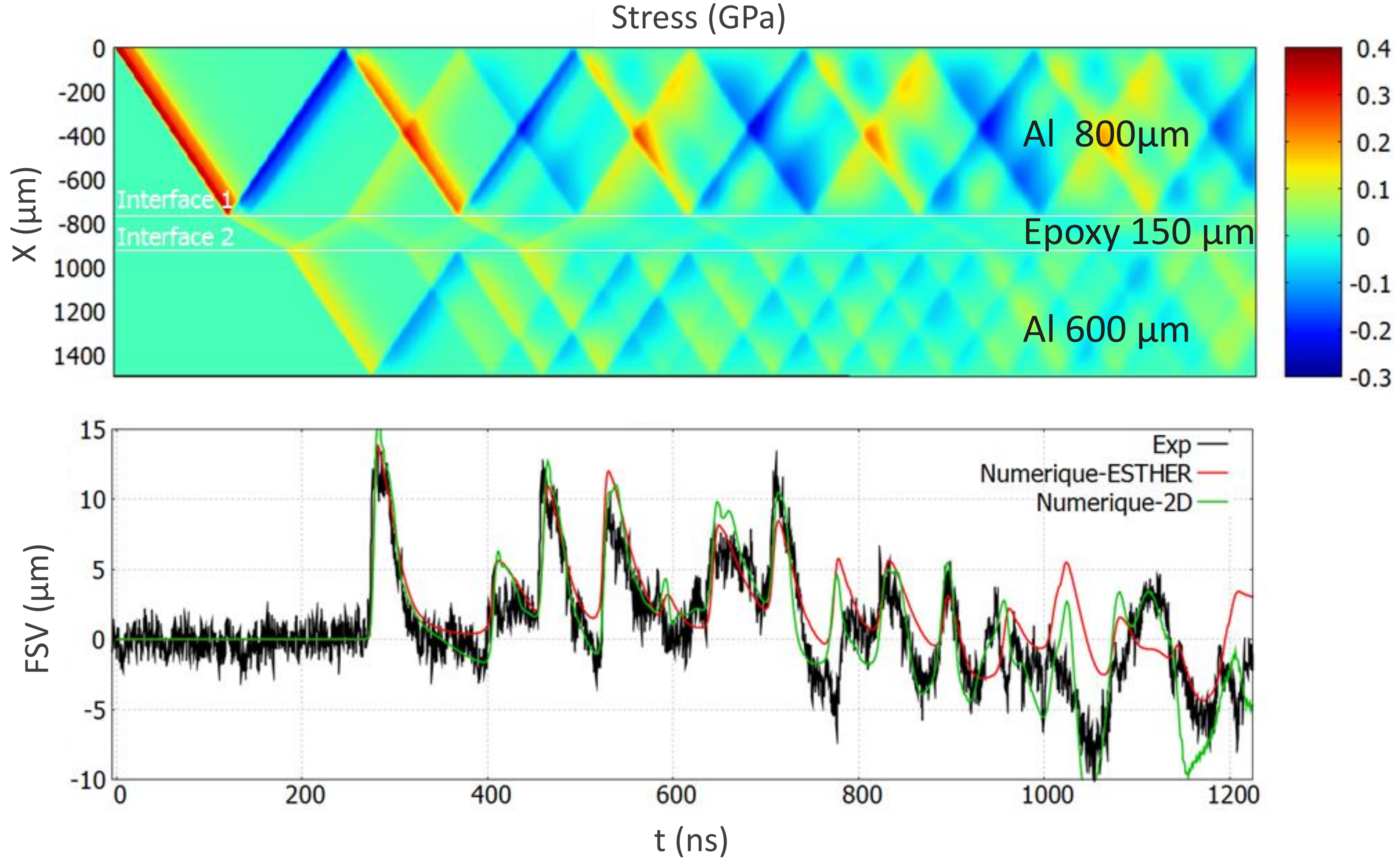

Comparison between static and LASAT mechanical tests

Damage thresholds measurements for 3 bond strength levels

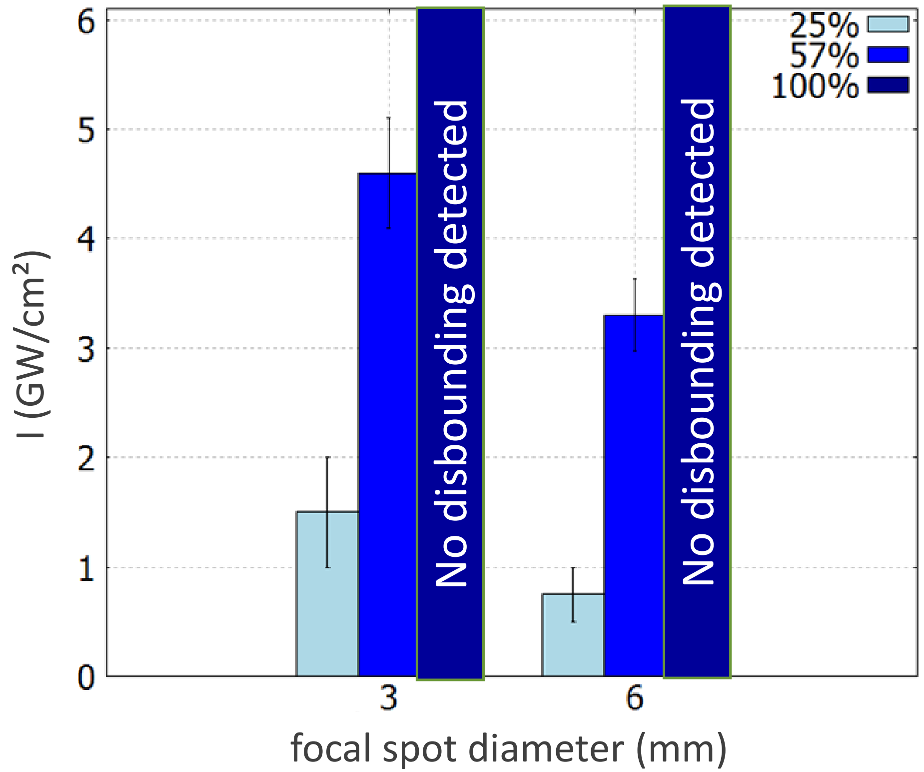

Numerical simulations : I(GW/cm²) → P(MPa)

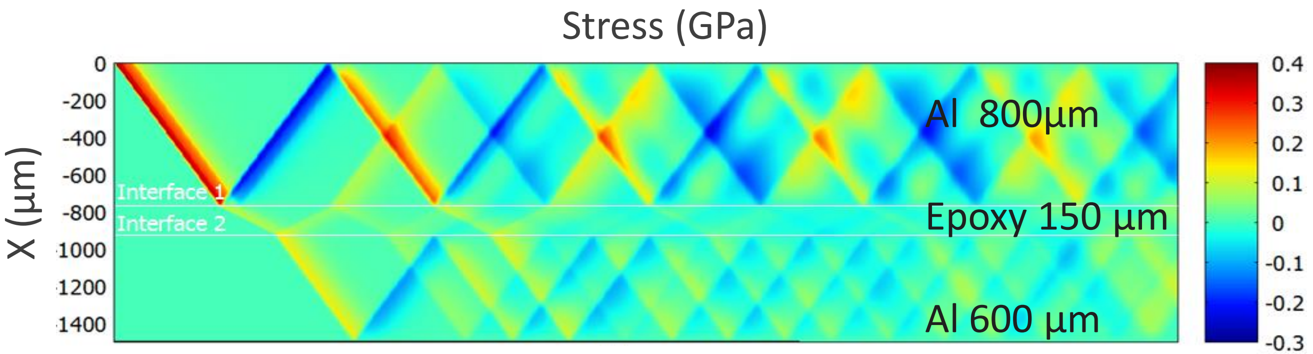

	σthreshold,LASAT	σthreshold, static
Correct Bond	> 390 MPa	62,7 MPa (+/- 3,2 MPa)
Weak Bond (High)	350 MPa	36 MPa (+/- 3,6 MPa)
Weak Bond (Low)	175 MPa	15,8 MPa (+/- 3,3 MPa)

X10

* S. Bardy thesis (2017)

Perspectives

Improvement of material properties for hydrodynamic codes

- WDM domain : everything needs to be improved ! (EOS, conductivities, optical properties, etc.)
- Two temperature model in solid/WDM domain (g_{ei}, C_e, K_e, optical properties, …)
- How to mix solid/WDM/plasma data ?

2D effects for vacuum and confinement regimes

- Temperature and density time-resolved measurements in the blow-off plasma
- How to address laser-mater interaction and material behavior in 2D dimensions ?

Thank you for your attention